



The distribution and abundance of planktonic foraminifera under summer sea-ice in the Arctic Ocean

Flor Vermassen^{1,2}, Clare Bird³, Tirza M. Weitekamp^{1,2}, Kate F. Darling^{3,4}, Hanna Farnelid⁵, Céline Heuzé⁶, Allison Y. Hsiang^{1,2}, Salar Karam⁶, Christian Stranne^{1,2}, Marcus Sundbom^{2,7}, Helen K. Coxall^{1,2}

¹Department of Geological Sciences, Stockholm University, Stockholm, Sweden

²Bolin Centre for Climate Research, Stockholm University, Stockholm, Sweden

³Biological and Environmental Sciences, Faculty of Natural Sciences, University of Stirling, Stirling, United Kingdom

⁴School of GeoSciences, University of Edinburgh, Edinburgh, United Kingdom

10 ⁵Centre for Ecology and Evolution in Microbial Model Systems - EEMiS, Linnaeus University, Kalmar, Sweden

⁶Department of Earth Sciences, University of Gothenburg, Gothenburg, Sweden

⁷Department of Environmental Science, Stockholm University, Stockholm, Sweden

Correspondence to: Flor Vermassen (flor.vermassen@geo.su.se)

15

Abstract. Planktonic foraminifera are calcifying protists that represent a minor yet important part of the pelagic microzooplankton. They are found in all of Earth's ocean basins and are widely studied in sediment records to reconstruct climatic and environmental changes throughout geological time. The Arctic Ocean is currently being transformed in response to modern climate change, yet the effect on planktonic foraminiferal populations is virtually unknown. Here we provide the first systematic sampling of planktonic foraminifera communities in the 'high' Arctic Ocean – here defined as areas north of 80°N – in a broad region located between northern Greenland (Lincoln Sea with adjoining fjords and the Morris Jesup Rise), the Yermak Plateau, and the North Pole. Stratified depth tows down to 1000 m using a multinet were performed to reveal the species composition and spatial variability of these communities below the summer sea-ice. The average abundance in the top 200 m ranged between 15-65 ind.m⁻³ in the central Arctic Ocean and was <0.3 ind.m⁻³ in the shelf area of the Lincoln Sea. At all stations, except one site at the Yermak Plateau, assemblages consisted solely of the polar specialist *Neogloboquadrina pachyderma*. It predominated in the top 100 m, where it was likely feeding on phytoplankton below the ice. Near the Yermak Plateau, at the outer edge of the pack ice, rare specimens of *Turborotalita quinqueloba* occurred that appeared to be associated with the inflowing Atlantic Water layer. Our results indicate that the anticipated turnover from polar to subpolar planktonic species in the Arctic Ocean has not yet occurred, in agreement with recent studies from the Fram Strait. The dataset will be a valuable reference for continued monitoring of the abundance and composition of planktonic foraminifera communities as they respond to the ongoing sea-ice decline and the 'Atlantification' of the Arctic Ocean basin. Additionally, the results can be used to assist paleoceanographic interpretations, based on sedimented foraminifera assemblages.

20
25
30



1 Introduction

35 Planktonic foraminifera are unicellular protists that form an important component of the pelagic biome. Their calcareous tests are common in the sediment record and are widely used as tracers of climatic and oceanographic conditions throughout geological time (Schiebel & Hemleben, 2017). To understand the response of foraminiferal communities to climatic change, a thorough understanding of their ecology is required. This is crucial for correctly interpreting temporal and spatial variations of foraminiferal assemblages and their geochemical signatures. One region that is vastly understudied with respect to its
40 planktonic foraminifera is the high Arctic Ocean (here defined as the ocean areas north of 80°N). With sea-ice retreating rapidly (Meier & Stroeve, 2022) and Atlantic waters increasingly influencing the Arctic domain (a process dubbed 'Atlantification'; Polyakov *et al.*, 2017), pelagic ecosystems are expected to be affected significantly (Brandt *et al.*, 2023). While the footprint of these processes on planktonic foraminifera communities is unknown to date, a recent meta-analysis suggests that the increased export of sea-ice through the Fram Strait is currently playing a key role in blocking the flux of
45 subpolar planktonic foraminifera towards the high Arctic Ocean (Greco *et al.*, 2022). It is anticipated that once this export ceases (i.e. essentially when the Arctic Ocean becomes seasonally ice-free), subpolar species will be able to rapidly invade the high Arctic Ocean (Greco *et al.*, 2022).

Baseline information and monitoring of planktonic foraminifera is needed to assess the impacts of the unfolding changes, especially in the sea-ice dominated high Arctic Ocean. Yet, knowledge of resident pelagic communities in the remote,
50 perennially ice-covered regions is minimal. Thus far, most studies have documented living planktonic foraminifera from the Arctic region stemming from areas within, or near, the seasonal sea-ice zone or near sea ice that is exported through the Fram Strait (Carstens *et al.*, 1997; Volkmann, 2000; Darling & Wade, 2008; Pados & Spielhagen, 2014; Fig. 1). These studies show that *Neogloboquadrina pachyderma* and *Turborotalita quinqueloba* are the dominant species in these regions, with occasional traces of *Globigerinita uvula* and *Globigerinita glutinata*. Only two previous studies have reached sites
55 located far into the perennial ice pack; this includes sampling stations at the Alpha Ridge at ca. 83°N (Bé, 1960) and stations up to 86°N in the Nansen Basin (Carstens and Wefer, 1992). Bé (1960) observed assemblages consisting only of *N. pachyderma*, at concentrations ranging 0-2.4 ind.m⁻³ at depths down to 500 m (single net). However, due to the large mesh size of the sampling net (200 µm) used in Bé's study, the results are not directly comparable to more recent work, which emphasizes the need for small net mesh sizes in the Arctic Ocean, ideally 63 µm, to sample juvenile *N. pachyderma* and,
60 potentially, subpolar species such as *T. quinqueloba*. This is important because *T. quinqueloba* are rather small in the Arctic region (Kandiano & Bauch, 2002; Vermassen *et al.*, 2023), and thus could be missed without the correct sampling approach. In general, the extent to which *T. quinqueloba* occurs in the central Arctic Ocean is a topical question. Two earlier plankton tow transects crossing the Nansen Basin found that *T. quinqueloba* decreased from ca. 30% of the standing stock at 81°N to 2-15% at 86°N (Carstens and Wefer, 1992). Importantly, these individuals were considered to have been transported along
65 the Atlantic Water flow path (i.e. branches of the West Spitsbergen current), and are not resident reproducing populations. Rather, the regions where they reproduce were thought to be located further south (Carstens and Wefer, 1992).



Here, we report the assemblage composition and depth distribution of planktonic foraminifera from eight vertical multinet hauls conducted in ice-covered waters in the high Arctic Ocean in late summer 2021 (*SAS ODEN21*). This is supplemented with ten plankton hauls performed in the Lincoln Sea and adjoining fjords (Petermann Fjord and Sherard Osborn Fjord),
70 conducted in late summer of 2019 (*RYDER19*). The aim of our study was threefold. First, we aimed to provide a snapshot of the standing stock of planktonic foraminifera underneath the perennial ice cover (summer sea-ice; Fig. 2) and test whether subpolar species such as *T. quinqueloba* were present. Second, we investigated the relationship between ambient environmental conditions and the observed planktonic foraminifera distribution patterns in order to gain a better understanding of the factors that control planktonic foraminifera abundance and species composition. Third, we used an
75 automated approach to extract and analyse morphometric data and explored whether this data could reveal clues regarding the population dynamics and, perhaps, the life history of *N. pachyderma*.

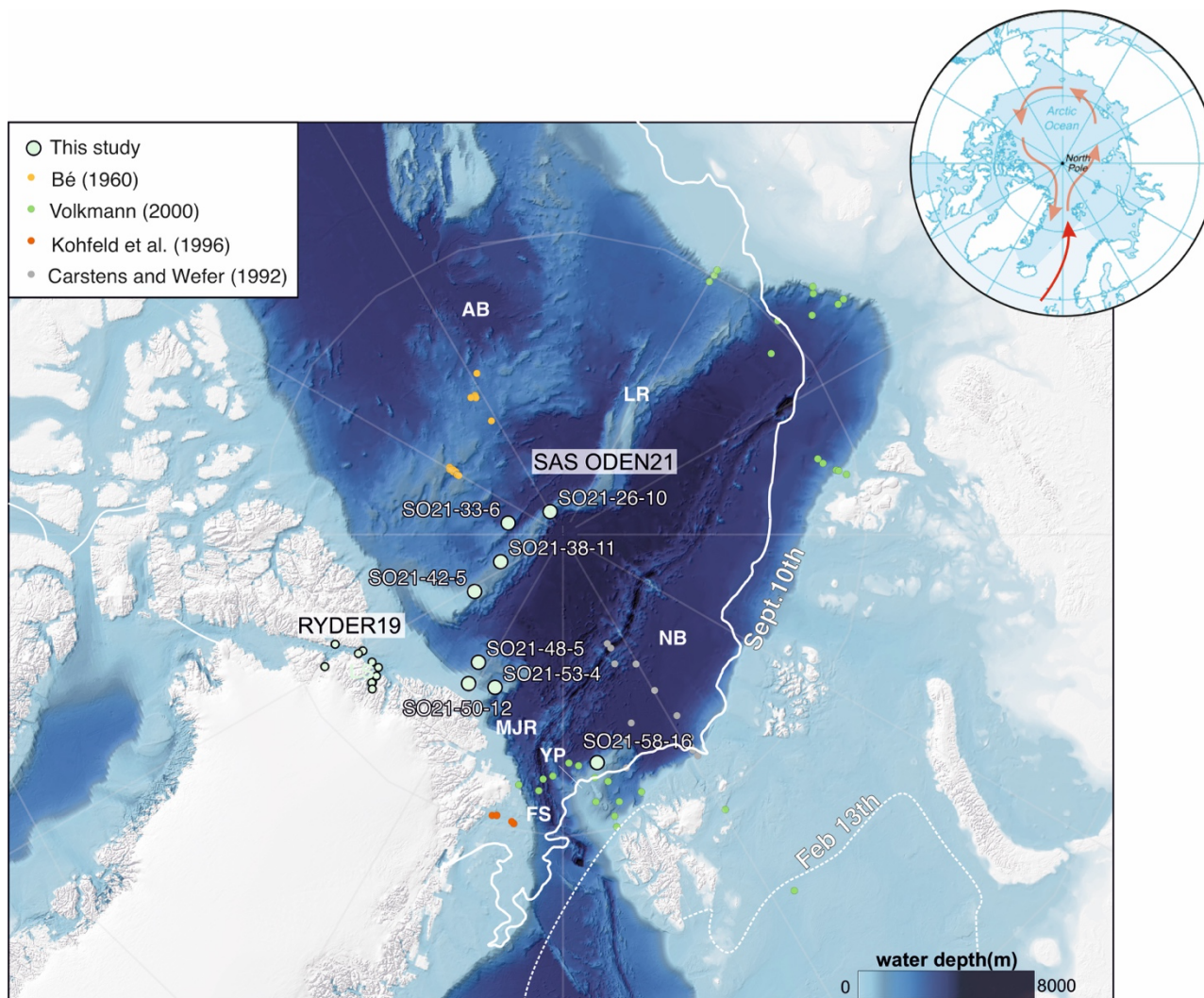
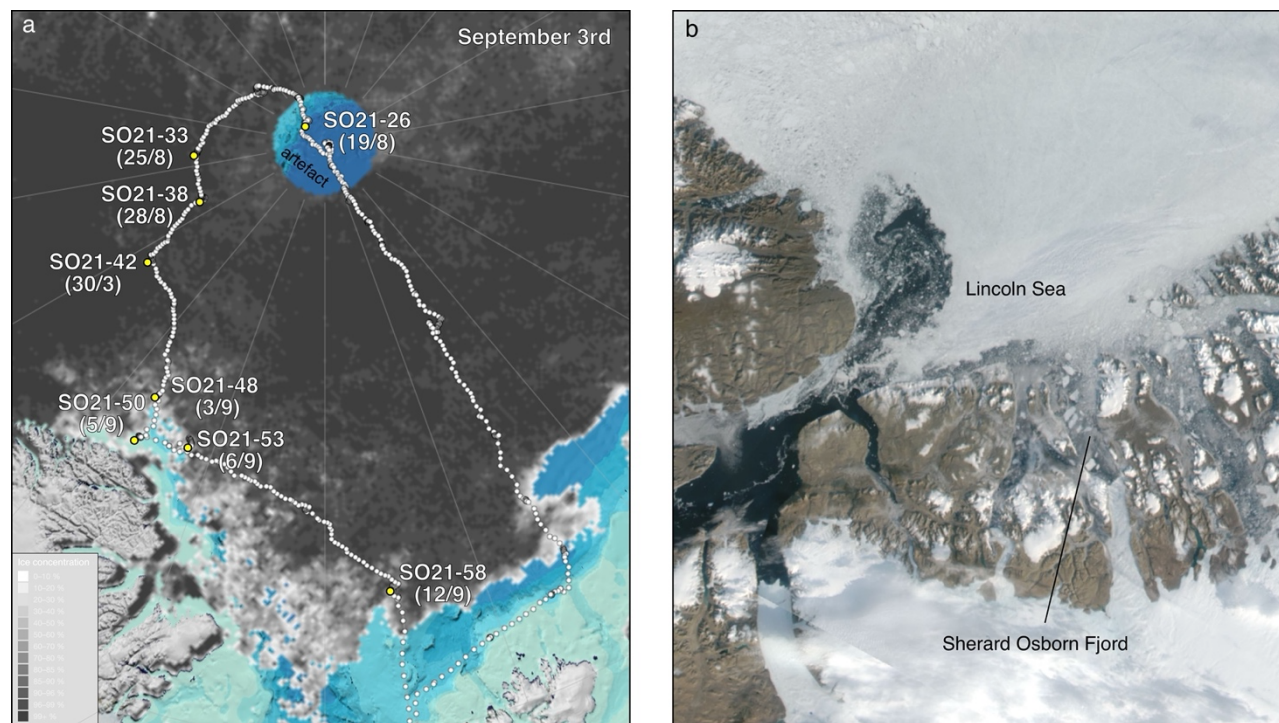


Figure 1: Bathymetric map of the Arctic Ocean (Jakobsson et al., 2020) with sampling stations obtained during the SAS ODEN 2021 and RYDER 2019 expeditions (this study) and previous foraminifera sampling sites carried out north of 80°N. Full station names and coordinates of sampling sites are listed in Table 1. LR = Lomonosov Ridge, MJR = Morris Jesup Rise, YP= Yermak Plateau, FS = Fram Strait, LS = Lincoln Sea. Inset figure in the upper right shows the track of warm Atlantic waters (red arrows) into the central Arctic Ocean, as they subduct under cooler and fresher waters. Sea ice extent on February 13th and September 10th in 2021 are also indicated (data US NIC).

80



85 **Figure 2:** a) Map displaying sea ice conditions during the expeditions SAS ODEN21 on September 3rd 2021, together with sampling sites. Sea ice data is from University of Bremen, visualised via <https://oden.geo.su.se/map/>. b) Modis satellite image (September 3rd 2019), displaying general ice conditions during RYDER19 expedition. Thick, multi-year sea ice covered most of the Lincoln Sea, whereas open water (with icebergs) was present in the fjords of north Greenland.

2 Methods

90 2.1. Sampling strategy

This study is based on two sampling campaigns conducted in the Arctic Ocean with Icebreaker Oden: the Synoptic Arctic Survey Expedition (hereafter *SAS ODEN21*) and the Ryder 2019 expedition (hereafter *RYDER19*). Multinet sampling was conducted during the *SAS ODEN21* (Snoeijs-Leijonmalm et al., 2022; Fig. 1), whereas single net plankton hauls were conducted during *RYDER19* (Jakobsson et al., 2020; Fig. 1). During *SAS ODEN21*, multinet water column sampling was conducted at eight stations from August 19th to September 11th 2021 at various times during the day under continuous daylight (midnight sun; Table 1). Sample sites include the central Lomonosov Ridge (located 100 km south from the North Pole), the Makarov Basin, the southern Lomonosov Ridge, the area north of Greenland (Morris Jesup Rise), and the Yermak Plateau (Fig. 1). A multinet (Hydro-Bios Multi Plankton Sampler MultiNet®, Type Midi) with surface area of 0.25 m² was

95



used. The net mesh was 55 μm , and the mesh of the cod end was 50 μm . Net clogging was not an issue in the ice-covered
100 Arctic Ocean where productivity and plankton standing stocks are relatively low compared to other ocean regions.

At each station, the bow of the ship was parked in the ice and plankton nets were deployed from the aft deck, i.e. in areas
where the ice had been broken up by the ship. The area where the cable and net enter the water is kept free from incoming
ice by water cannons located near the edge of the aft deck – these spray the ocean surface and create a small current away
from the ship. Larger pieces of incoming ice were manually diverted using large boathooks to push away incoming ice.

105 By default, the multinet was lowered to and hauled from 1000 m depth unless the site was shallower, in which case the
multinet was hauled from ca. 20 m above the seafloor (Table 1). The default sampling depth intervals were 1000–500 m,
500–200 m, 100–50 m and 50–0 m. The upwards towing speed was 0.5 m/s, and towing was paused for approximately one
minute at the start of each sampling interval. After deployment, the samples were transferred from the cod ends to
containers. Samples were then pipetted onto a glass petri dish and visualised under the microscope (ZEISS Stemi 508).
110 Planktonic foraminifera individuals were picked onto microfossil slides using a combination of pipettes and brushes.
Samples that could not be picked shipboard due to time constraints were preserved in an EtOH solution and picked post-
cruise at Stockholm University. All planktonic foraminifera individuals were identified and counted. At station SO21-26-10,
the colour of cytoplasm-bearing individuals was noted and counted. The concentration of planktonic foraminifera (number of
individuals per cubic meter filtered water) was calculated via the formula:

115
$$\frac{n}{a \cdot d}$$

where n = number of individuals counted for a given the depth interval, a = the surface area of the net, and d = the length of
the sampled depth interval.

A smaller scale sampling program involving more opportunistic sampling was conducted during *RYDER19* held during
August 9th - September 3rd 2019 (Table 1; Jakobsson *et al.*, 2020). A simple plankton net (60 cm diameter net opening, 83
120 μm mesh), with a 13 kg weight attached, was lowered to a depth of 300 m and hauled vertically at a rate of ca. 0.2 m/s,
sampling the entire depth interval at ten stations. On deck, the net content was washed out of the cod end with filtered
seawater into a storage container. Foraminifera that settled to the bottom of the container were picked from the concentrate.
For comparison with our data, concentrations of *N. pachyderma* in the Nansen basin reported by Carstens and Wefer (1992)
were calculated by multiplying their reported % of *N. pachyderma* with their reported numbers of total planktonic
125 foraminifera concentrations. Concentrations of *N. pachyderma* in the top 200 m of other studies were calculated from the
original data available online.

2.2. Test size and morphometric analysis

Picked individuals ($N=15\ 381$) were imaged with a Leica M205 C microscope – one photo was taken for each square on the
microfossil slide. Individuals were segmented from these images using the ‘segment’ module of AutoMorph (Hsiang *et al.*,
130 2017; development version available at <https://www.github.com/ahsiang/AutoMorph>), which automatically separates and



extracts individual imaged objects using traditional image processing methods. As the lighting conditions were set manually and could change between images, all images were initially processed under ‘Sample’ mode in AutoMorph to determine the optimal parameters (i.e., threshold value and min./max. size of legitimate objects) for segmenting objects in each image. Threshold values tested ranged from 0.10 to 0.79 and size ranged from 50 to 500 μm depending on individual image conditions. Optimal parameter values were chosen to maximize the number of individuals correctly identified. A pixel size of 2.571 μm was used for both the x- and y-axes based on output from the Leica microscope. The images were then processed under ‘Final’ mode with the optimal parameter values using batch-processing mode to obtain individual cropped images of each specimen. Incorrectly identified non-foraminifer material (e.g., organic fluff and junk images of the background texture of the slides) were removed manually in post-processing. All specimen images were compiled and then processed using the ‘run2dmorph’ module of AutoMorph. This module detects the outlines of individuals and then automatically extracts morphometric measurements such as major/minor axis length, perimeter length, area, etc. Default values were used for all input parameters to ‘run2dmorph’.

2.3. CTD, chlorophyll *a* and nutrients

Conductivity-Temperature-Depth (CTD) measurements for *SAS ODEN21* were obtained using two standard Seabird SBE911 plus systems, one “shallow” (maximum 1000 m depth) and one “deep” (full-depth), each with dual sensors to measure temperature and salinity, and single sensors to measure pressure and dissolved oxygen concentration. For more information about hydrographic operations, we refer to the cruise report provided by Snoeijs-Lejonmalm et al. (2022). All sensors have been pre- and post-cruise calibrated by the Swedish Polar Research Secretariat. Salinity and Oxygen were further calibrated against sample data collected from the bottles. Salinity samples from the deep stations were analysed post-cruise using a Guildline Autosal salinometer and IAPSO standard seawater at the GEOMAR, Germany. Dissolved oxygen was determined onboard using an automatic Winkler titration setup with UV detection (Scripps Institute of Oceanography Oxygen Titration System version 2.35m). The fully calibrated data sets are freely available at the PANGAEA database (Heuzé et al., 2022a; sensor data) and (Heuzé et al., 2022b; bottle data).

CTD measurements during the Ryder 2019 expedition were made with a Seabird SBE911 plus with dual temperature (SBE 3) and conductivity (SBE 04C) sensors. The CTD was equipped with a dissolved oxygen sensor (SBE 43), turbidity sensor (WET labs ECO), fluorescence sensor (WET Labs ECO-AFL/FL) and altimeter (BENTHOS ALTIMETER PSA-916D). The CTD was mounted on a 24 Niskin bottle (12 liters) rosette. All sensors were pre- and post-cruise calibrated by the Swedish Polar Research Secretariat. The data set is available at the Bolin Centre Database (Stranne et al., 2020).

On the *SAS ODEN21* expedition, seawater was collected using a SBE rosette system equipped with 22 Niskin bottles (12 L), that was deployed from the bow of the ship. The bottles were closed at predefined depths (10, 20, 30, 40, 50, 75, 100, 125, 150, 200, 250, 300, 400, 500, 700, 1000 m, following the international SAS protocol) during the return of the CTD from the bottom. Directly after the CTD was back on deck, water samples (100 ml) were taken from each Niskin bottle using clean sampling methods. As soon as possible after sampling, typically on the same day, concentrations of the macro-nutrients



phosphate, nitrate+nitrite, ammonium, and silicate (PO_4 , NO_3+NO_2 , NH_4 , and SiO_4) were determined colorimetrically on
165 board using a four- channel continuous flow analyser with photometric detection (QuAAtro39, SEAL Analytical). The
instrument was set up to use QuAAtro Methods No. Q-064-05 Rev. 8, Q-119-11 Rev. 2, Q-069-05 Rev. 8 and Q-066-05
Rev. 5 for PO_4 , NO_3+NO_2 , NH_4 , and SiO_4 , respectively. These methods largely correspond to standard methods SS-EN ISO
15681-2:2018, SS-EN ISO 13395:1996, SS-EN ISO 11732:2005 and SS-EN ISO 16264:2004. Each analysis run included
standards freshly prepared from stock solutions, certified reference material (VKI QC SW4.1B and VKI QC SW4.2B) and
170 solutions for automatic baseline/drift correction.

Chlorophyll *a* was sampled at the defined depths down to 500 m. Samples were kept in 4,7 L brown bottles at low ($\sim 4^\circ\text{C}$)
temperatures until processing. Size fractionated samples were attained using $2.0\ \mu\text{m}$ polycarbonate filters (diameter 25 mm)
as well as $0.3\ \mu\text{m}$ glass fibre filters (Advantec®, diameter 25 mm). Filters were placed inside Swinnex capsules and serially
connected at the end of a peristaltic pump system. Seawater was divided into two 2 L bottles to collect replicate samples and
175 was pumped through the system at a low pump rate (30 rpm) to ensure cell integrity on the filters. Seawater was filtered
either until the filter system clogged or 2 L of seawater passed through. Filters were immediately placed in test tubes with
2.5 mL 95% EtOH and stored in the dark at room temperature for >16 hours before measurement on a Trilogy Fluorometer
(Turner, USA). The instrument was calibrated using a standard from *Anacystis nidulans* (Sigma-Aldrich).

3 Results

180 3.1. Environmental conditions

3.1.1. Oceanography

Overall, in the upper 1000 m analysed here, three distinct water masses were present throughout the expeditions, as expected
(e.g. Rabe et al. 2021; Rudels 2000). In the top 10-150 m, a cold (ca. -1.5°C) and low salinity (29-34 g/kg) water mass was
present (Figs. 3 and 4). This layer is commonly referred to as the Polar Surface Water (PSW), defined as $\sigma_\theta < 27.7\ \text{kg m}^{-3}$
185 (Rudels *et al.*, 2008). Below this, the Atlantic Water layer, characterised by higher temperatures ($>0^\circ\text{C}$) and relatively high
salinity ($>34.9\ \text{g/kg}$), occupied 500-800 m depending on the casts. This water mass is derived from North Atlantic currents,
which subside beneath the cold polar waters as they enter the ice-covered central Arctic Ocean. At station SO21-26-10, in
the North Pole area, the Atlantic water layer was markedly warmer ($T_{\text{max}}=1.48^\circ\text{C}$) than at the other sites on the Lomonosov
Ridge and Morris Jesup Rise, implying a more proximal branch of inflowing Atlantic Waters (Figs. 3 and 4). At station
190 SO21-58-16, the PSW was much thinner and Atlantic-derived waters were present between 100-750 m depth (Fig. 4) and
warmer ($T_{\text{max}} = 1.64^\circ\text{C}$). Below the Atlantic Water lies the deep water, characterized by temperatures lower than 0°C but
with a salinity that remains high.

Similar hydrographic conditions are generally found in the area north of Greenland. In the Sherard Osborn Fjord, however,
the shallowest 10 m of the PSW was ‘dammed’ by the heavy sea-ice conditions outside the fjord, in the Lincoln Sea, which



195 led to highly elevated temperatures (reaching 4 °C) low salinities (< 15 g kg⁻¹), and low associated Chl-a concentrations within the fjord (Stranne *et al.*, 2021). The Atlantic Water in the north Greenland fjords is to some extent influenced by subglacial runoff and melting from marine-terminating glaciers forming glacially-modified water. This was particularly evident inside the Sherard Osborn Fjord where local bathymetry influences the deep water circulation inside the fjord (Jakobsson *et al.*, 2020b; Nilsson *et al.*, 2023).

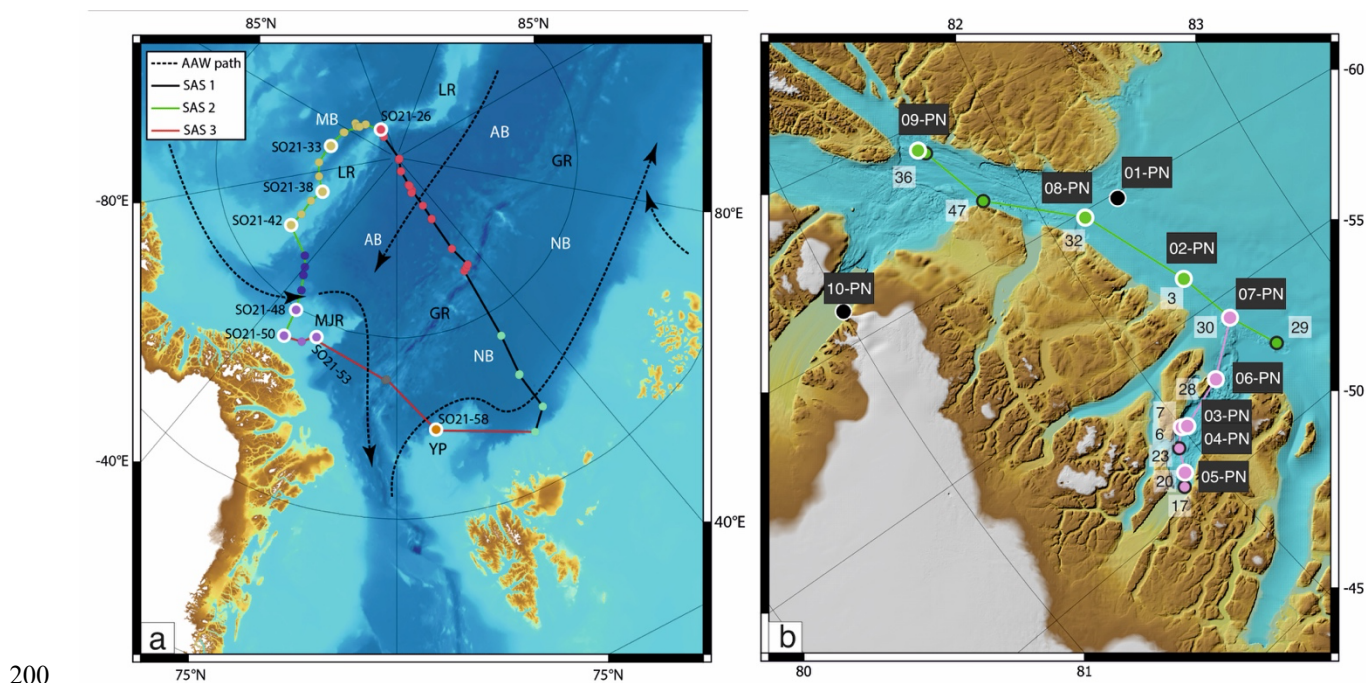


Figure 3: A) Map showing locations of CTD stations during SAS ODEN21 and transects depicted in Figure X. Sites with white circles depict combined CTD and foraminifera sampling. B) Map showing locations of foraminifer sampling stations (white text, black label: “xx-PN”) and CTD stations (black text, white label) during RYDER19 and transects depicted in Figure 3. Sites with white circles depict combined CTD and foraminifera sampling sites.

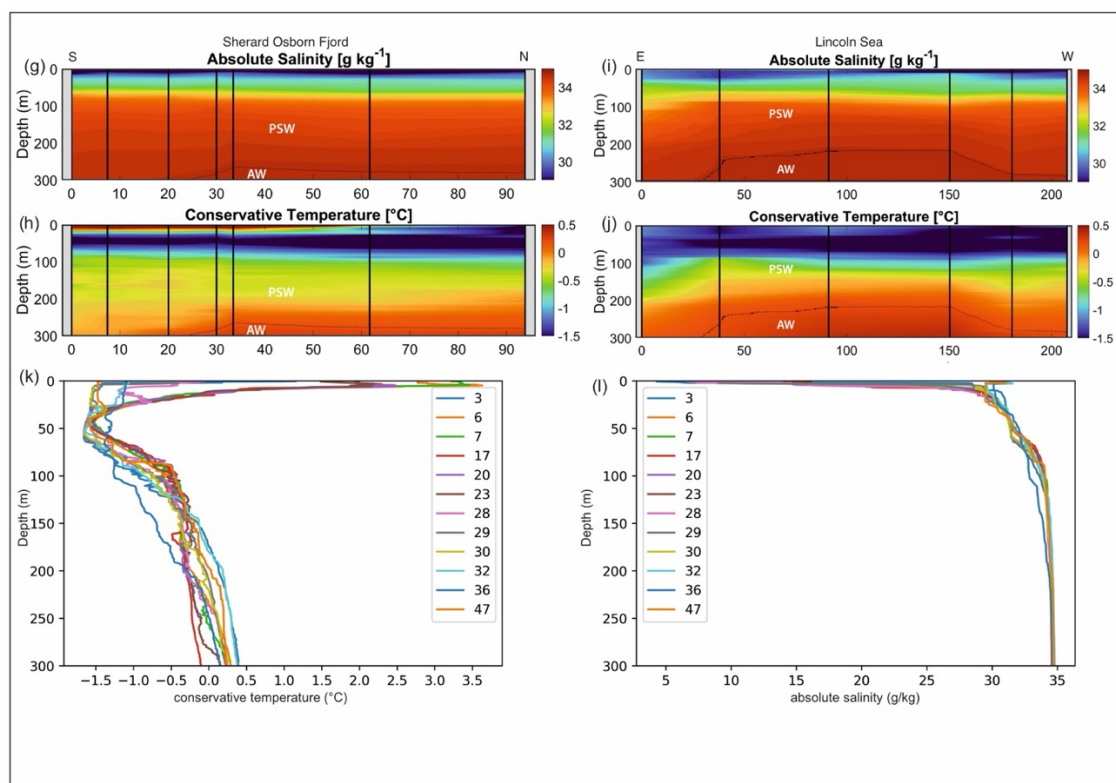
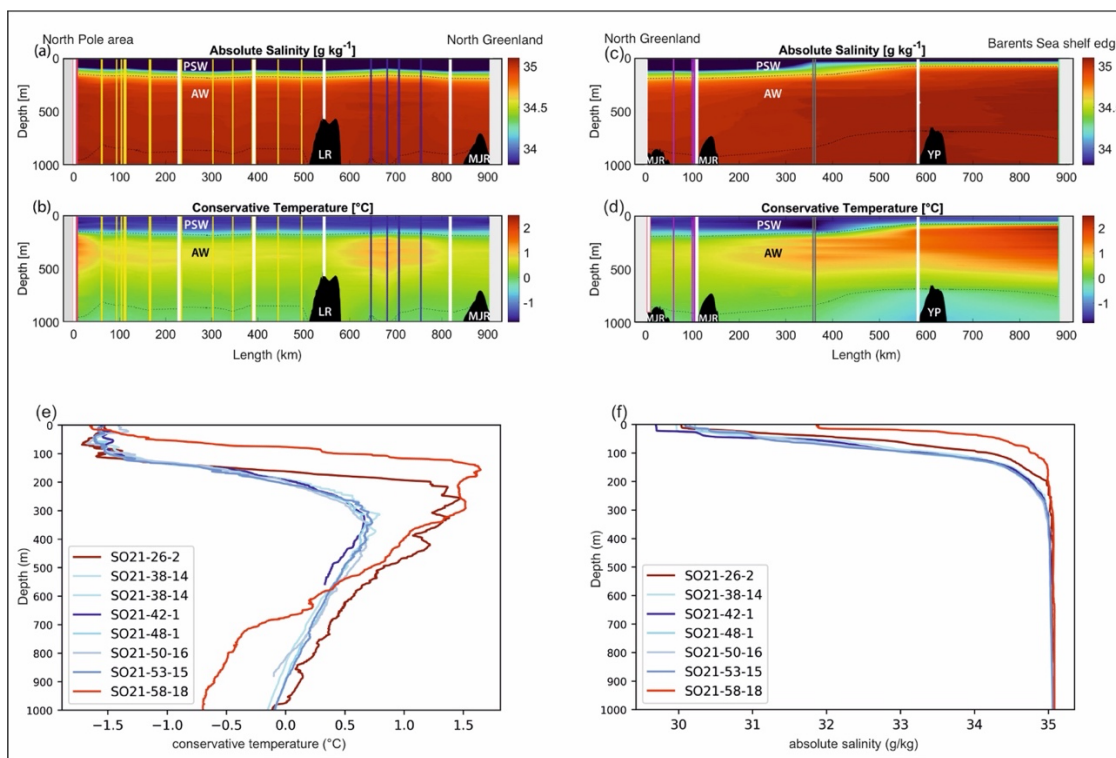




Figure 4: Oceanographic data (temperature and salinity) obtained during SAS ODEN 21 (a to f) and RYDER19 (g to l). Transects of temperature (b,d,h,j) and salinity (a,c,g,i) are presented. Temperature profiles (e, k) and salinity profiles (k,l) combined for each expedition are also presented. Salinity and temperature profiles are shown separately for the Lincoln Sea region and Sherard Osborn Fjord in Figures A2 and A3.

210 3.1.2. Sea ice

All of the stations sampled during *SAS ODEN21* were characterized by intense sea-ice conditions (ice coverage >95 %) (Fig. 2). Sea-ice thickness estimates derived from ice cores obtained near the sampling stations samples ranged from 1.1 to 2.6 m (average of 1.8 m; Snoeijs-Leijonmalm, 2022). However, these observations exhibit a bias towards greater ice thickness as sites with thicker ice were selected for safety precautions and ship stability. Therefore, ‘real’ regional average ice thickness reported here should be considered significantly lower.

Another factor that has a possible effect on planktonic foraminifera abundance is the distance to the sea-ice edge. For *SAS ODEN21*, Stations SO21-26-10, SO21-33-6, SO21-38-11, SO21-42-5 were located well within in the Arctic ice pack, > 300 km from the nearest sea ice edge, while stations SO21-50-12, SO21-53-4, and SO21-58-16 were located rather close to the ice edge (<50 km). While station SO21-48-5 was located relatively close to a narrow lead of open water, it was located about 80 km from the broader sea-ice edge/marginal ice zone (Fig. 2).

In the Lincoln Sea the ice cover generally consisted of very thick multi-year sea-ice, but areas bordering North Greenland and off Ellesmere Island were temporarily ice-free (Fig. 2). Sherard Osborn was free of sea-ice during the time of sampling, but with icebergs present.

3.1.3. Patterns of chlorophyll, nutrient and oxygen concentrations.

225 Concentrations of chlorophyll *a* were typically moderately high near the surface, increased with depth, and reached a maximum between 20-40 m water depth (Fig. 5). Chlorophyll *a* maximal values ranged between 0.11-1.10 µg/L. Below this, concentrations decreased, until they became negligible at about 50-70 m depth. At station SO21-58-16 no distinct subsurface chlorophyll *a* maximum was observed, instead, values were highest near the surface (top 10 m).

230 Concentrations of nitrate + nitrite (NO₂₃), phosphate (PO₄) and silicate (SiO₄), displayed comparable depth profiles overall, although there were some differences among stations in the top 200 m. From the surface and down to chlorophyll maximum, nutrients were strongly depleted, especially of NO₂₃ (Fig. 4). Between 50-150 m, a pronounced peak occurred at stations SO21-33 to SO21-53, typically with a maximum at around 75 m depth. This peak was much weaker at station SO21-26 where PO₄ and SiO₄ instead showed a minimum at around 100 m. At the Yermak plateau (station SO21-58-16), there was no subsurface maximum. Rather, there was a steep increase in nutrients concentrations down to 100 m. At greater depths, below 200 m, nutrient concentrations at all stations converged to very similar values.

Stations SO21-33 to SO21-53 share similar trends in oxygen concentration throughout the water column (Fig. 5). In the top 30 to 50 m of these stations, oxygen values stay broadly constant around 8.9 ml/l. Down to 100 m, values decreased rapidly



and remain constant at around 7.8 ml/l. At stations 26, values decline from 8.7 ml/l near the surface to 6.9 ml/l at 100 m, between 100-120 m values peak to 7.6 ml/l again and then remain constant at 6.9 ml/l below 120 m. At station SO21-58, oxygen values decline from 8.6 near the surface to 6.9 ml/l at 100 m, below which they remain constant.

The nutrient and oxygen profiles (Fig. 4), as well as the salinity profiles (Fig. 3), indicate the presence of the Transpolar Drift Stream at stations SO21-33 to SO21-53, whereas surface waters near the North Pole (station SO21-26) and particularly on the Yermak Plateau (station SO21-58) were less influenced by this major ocean current in 2021.

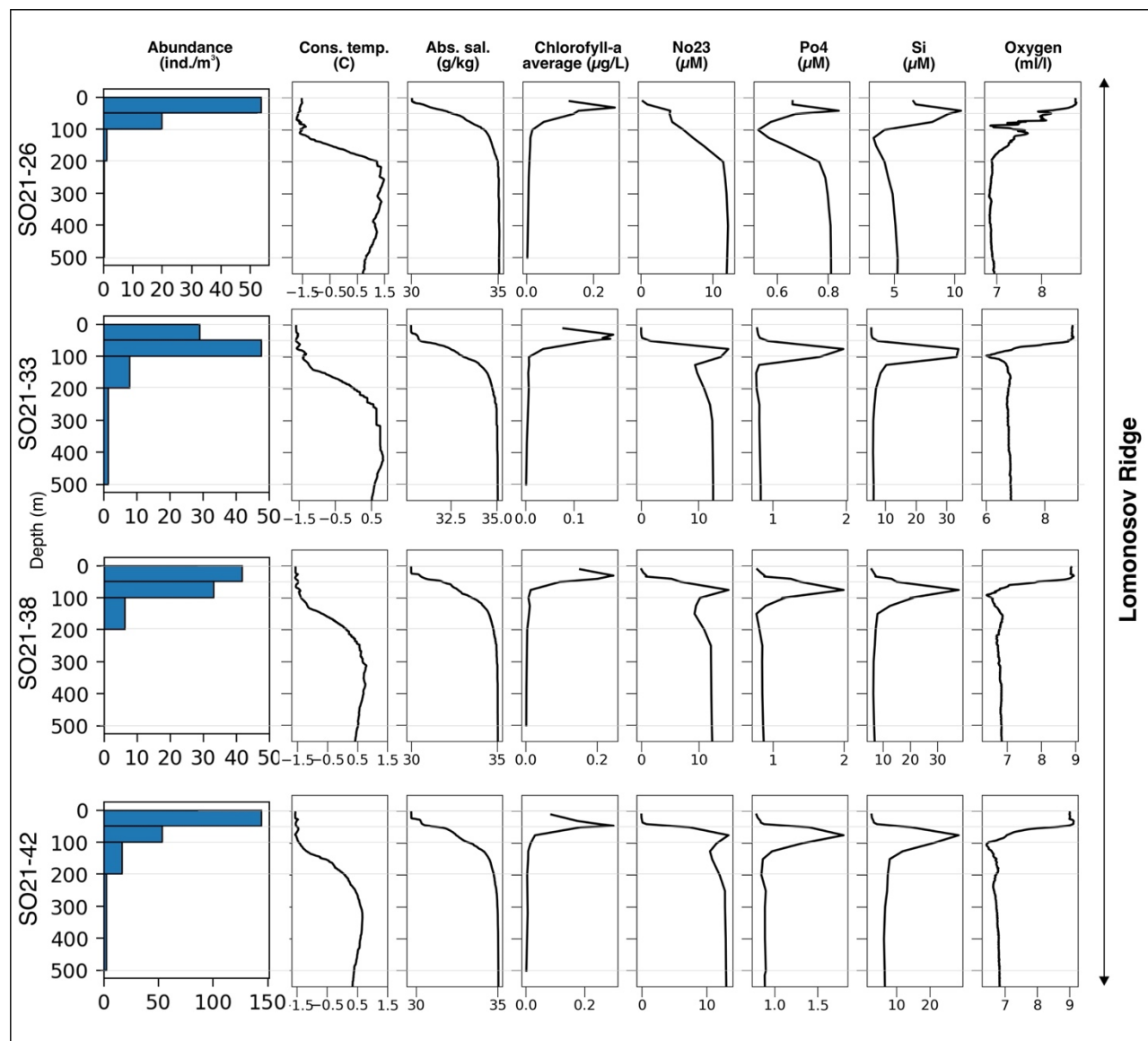
3.2. Planktonic foraminifera

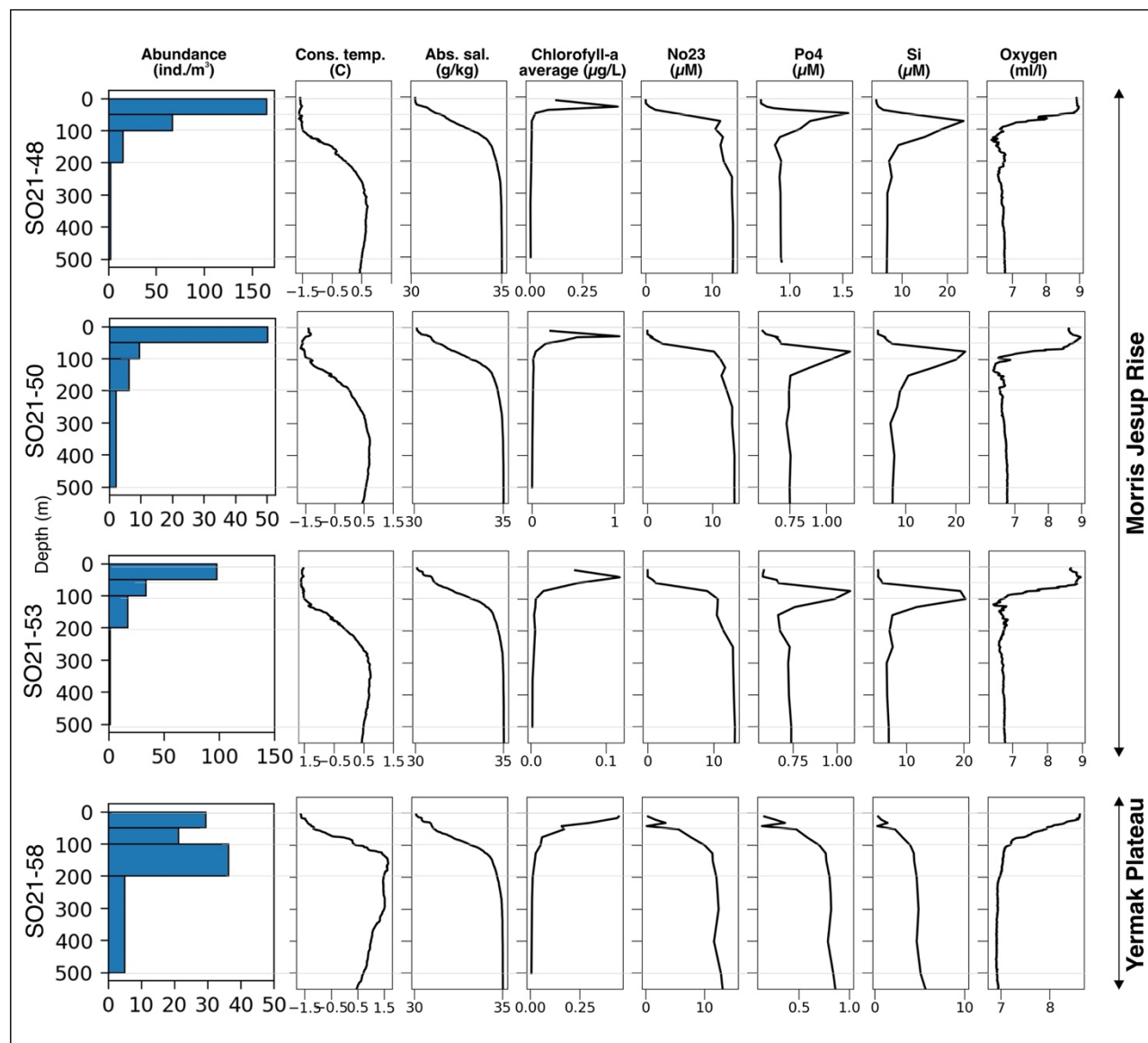
3.2.1. Spatial variability

The variability of average planktonic foraminifera concentration in the top 200 m was relatively high and varied between 18 and 65 individuals/m³ at sites located in the central Arctic Ocean (*SAS ODEN21*; Fig. 6). No obvious spatial trends in abundance were observed in the central Arctic Ocean data set. The concentration of individuals in the water column appears to be relatively low in the North Pole area (18 ind./m³; station SO21-16-10) and close to the north Greenland coast (19 ind./m³; SO21-50-12, ca. 60 km north of Cape Morris Jesup). Highest concentrations occurred at the southern end of the Lomonosov Ridge (Greenland side) and the northern tip of the Morris Jesup Rise (58 and 65 ind./m³ at SO21-42-5 and SO21-48-5, respectively; Fig. 6). In the Lincoln Sea, Ryder Fjord and Petermann Fjord, abundances were extremely low, with maximal abundances of ca. 0.3 ind./m³ (Fig. 6). Although generally low, it is noteworthy that concentrations in the shelf area of Lincoln Sea were higher than within the fjords. Near the front of Ryder glacier (station RYDER19-05PN), zero individuals were found.

3.2.2. Depth variability

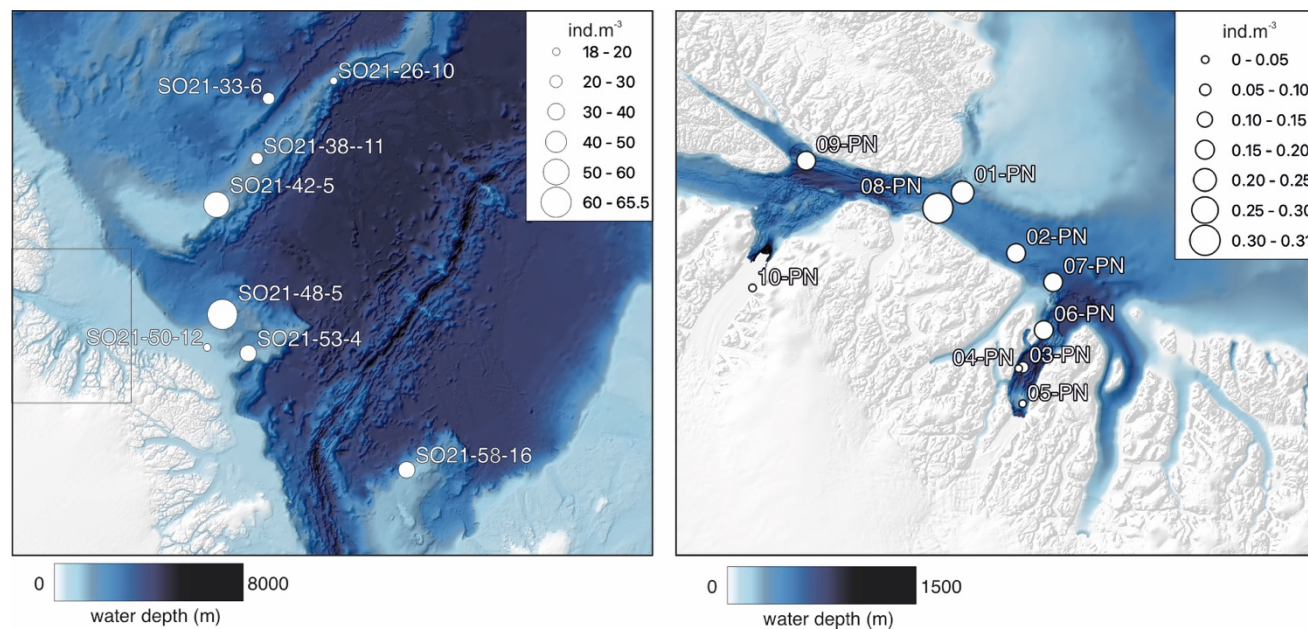
Overall, planktonic foraminifera concentrations were by far the highest in the top 50 m of the water column (Fig. 5). At 5 out of 8 stations in the central Arctic Ocean, the concentration of individuals in the top 50 m was more than double the concentration of individuals in the 50-100 m interval (Fig. 5). At station SO21-33-6, the concentration of individuals was higher in the 50-100 m depth interval than in the top 50 m (48 vs 30 ind./m³) and at SO21-38-11, the difference in concentration between the top 50 m and the 50-100 m depth interval was small (42 vs 36 ind./m³). At all stations, except SO21-58-10, the percentage of individuals living in the top 100 m was >65%. At all stations, depths >200 m recorded a low number of individuals (<5 ind./m³), comprising only a minor percentage of the total foraminiferal standing stock at each site. At station SO21-58-16, the depth distribution of foraminifera was different, with the maximal concentration of foraminifera present at 100–200 m, instead of in the top 100 m, with only 28% of the individuals living above top 100 m and 72% living below 100 m. Below 500 m, the concentration ranged between 0.03-3.75 ind./m³ (Fig. A1, not shown in Fig. 5 to facilitate better visual comparison with water column parameters).





270

Figure 5. Overview of planktonic foraminifera abundance in relation to environmental parameters at sampling station (SAS ODEN21). Thin horizontal grey lines indicate the limits of the sampled depth intervals. Blue bars represent abundance of *N. pachyderma*. At site SO21-58, *T. quinqueloba* was found at very low abundances below 100m, and the concentrations were lower than the line width of the bars. Note scale change of foraminifer abundance at different sites.



275

280

Figure 6: Left) Average abundance of planktonic foraminifera (ind.m^{-3}) in the top 200m for samplings stations obtained during SAS21. Thin box indicates general sampling area of RYDER19. Right) Average abundance of foraminifera (ind.m^{-3}) in the top 300m for sites sampled during RYDER 2019, except for stations 04 and 05, where sampling depths reached 408 and 250 m, respectively. Note that no individuals were found at station 05-PN. Note the difference in scale of the concentrations between the two panels.

3.2.3 Species composition and size distribution

At all stations, except SO21-58-16, the planktonic foraminifera assemblage was monospecific, consisting of *N. pachyderma* (Plate 1). At station SO21-58-16, a minor proportion of *T. quinqueloba* was encountered below 50 m, comprising 0.3%, 3.3% and 3.90% of the assemblage at the 50-100m, 200-500, and 500-1000m depth intervals, respectively (Plate 2).
 285 Specimens from *N. pachyderma* species were pristine and showed no signs of dissolution (Plate 1).

All *N. pachyderma* morphotypes ('Nps 1-5'; Eynaud *et al.*, 2009) were observed (Plate 1) – however a deeper analysis of morphotypes (e.g. morphotype distribution per depth interval), will be the topic of a follow-up study. In the relatively shallow water depths (the top 100 m) the majority of *N. pachyderma* were small (range of the mean maximal diameter in the top 50m = 124-141 μm ; average of all means in the top 50m = 134 μm ; Fig. 11) and lightly calcified, giving them a translucent appearance under a light microscope, with an appearance similar to 'Nps-5'. At the deeper levels (>200 m), specimens appeared to mostly belong to the more heavily calcified morphotypes 1 to 4 (see Introduction and Plate 1). The
 290 range of mean maximal diameter in the water depths below 500m was 164-261 micron, with an average of all means 202 micron (Fig. 11).



295 Cytoplasm-bearing shells were observed at all depths but were predominant in the top 100 m, whereas tests below 200 m
were mostly 'empty', i.e., they were colourless tests that were settling to the seafloor following reproduction. Interestingly,
the cytoplasm-bearing tests consisted of two types: red and yellow-green (Fig. 8). Some individuals consisted of both red-
and green-coloured chambers (Fig. 8). The cytoplasm colours transformed rapidly and after ca. 12 hours the relatively bright
colours had faded, hindering their discrimination. At station SO21-26-10, all tests could be rapidly picked and the colour of
their cytoplasm was noted immediately (Fig. 7). This revealed that the red-coloured individuals dominate the top 50 m, while
300 the green/yellow type were dominant in deeper waters. Due to time constraints, quantification of cytoplasm colour was not
feasible at other stations, although observations during picking confirmed this pattern.

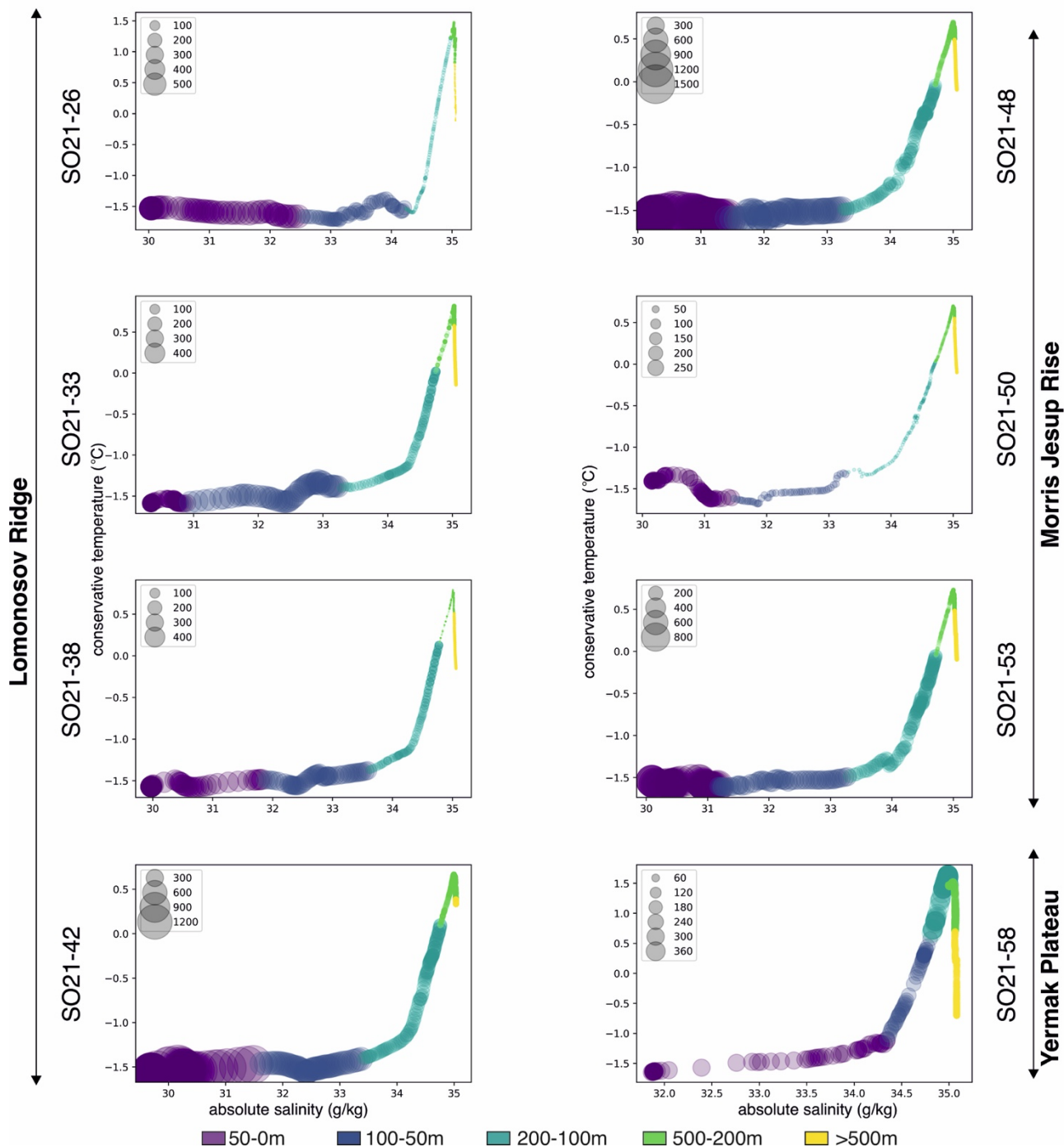
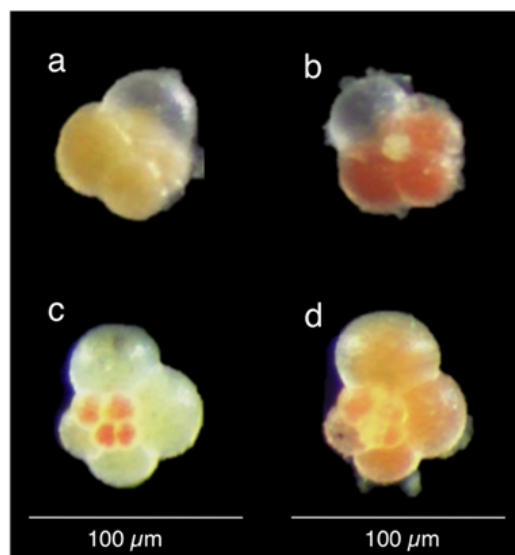
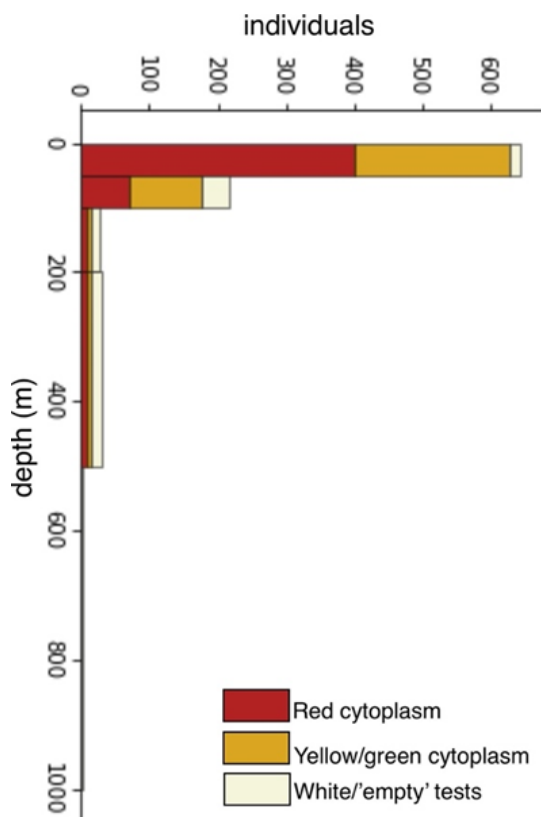


Fig. 7. Planktonic foraminifera abundance (individuals per m^3) plotted in the temperature-salinity space (*SAS ODEN21*). For each T-S data point, the average foraminifer abundance of the corresponding depth interval is plotted.



305

Fig. 8. Left) Counts of individuals at station 26-10, according to cytoplasm colour. Right) Example of (a) yellow/green, (b) red, and (c and d) mixed yellow/green-red coloured cytoplasm in living *N. pachyderma*.

4 Discussion

4.1. Current and future composition of planktonic foraminifera in the central Arctic Ocean

310 Our results show that *N. pachyderma* is the only species that currently lives and thrives beneath summer sea-ice in the region between the North Pole and North Greenland. A few occurrences of *T. quinqueloba* were found at the northern tip of the Yermak Plateau (SO21-58-16), proximal to the marginal ice zone at depths below 100 m (<4%). Our results are as expected, since *N. pachyderma* has long been considered the only true polar species that is capable of living in the ice-covered Arctic Ocean (Bé, 1960; Carstens & Wefer, 1992). *T. quinqueloba*, on the other hand, is known as a sub-polar species that thrives

315 in areas near the sea-ice edge, but is not known to reproduce under permanent ice, although it can survive for a limited time in ice-covered conditions (Carstens & Wefer, 1992; Volkmann, 2000; Zamelczyk *et al.*, 2021). In the study of Carstens and Wefer (1992), a significant number of *T. quinqueloba* were found in the Nansen basin (up to 55% south of 83°N and up to 15% north of 83°N), but these individuals were considered to have been advected along with Atlantic currents, with their



reproduction area being further south. More recently, a population of *T. quinqueloba* was observed underneath the growing
320 winter sea-ice of the seasonally ice-free Barents Sea in December (comprising 16–67% of the standing stock, the rest being
N. pachyderma) albeit at very low absolute concentrations ($<1.5 \text{ ind.m}^{-3}$; Zamelczyk *et al.*, 2021).

The Barents Sea is a hotspot for ‘Atlantification’ (Polyakov *et al.*, 2017) and it was suggested that the *T. quinqueloba*
population under the winter ice in the Barents Sea was probably not reproducing *in situ*, but rather had stayed in place after
reproduction in open waters and the subsequent onset of winter freezing. From these two studies, it could be anticipated that
325 the rare *T. quinqueloba* occurrences we observed near the Yermak Plateau – where Atlantic waters are present at relatively
shallow water depths ($T > 0^\circ\text{C}$ at 70 m) – can be explained as individuals that survived under the sea-ice but were not
actively reproducing. SEM images of *T. quinqueloba* reveal no intact spines, or even broken spine remains, which suggests
that these *T. quinqueloba* had been transported.

The absence of *T. quinqueloba* at sites located near the Lomonosov Ridge and north Greenland – located at higher latitude
330 and/or further along the path of Atlantic currents compared to Carstens and Wefer (1992) – demonstrates that *T. quinqueloba*
(or other sub-polar species) are not yet present in the central Arctic Ocean and do not survive advection to these sites. Thus,
despite the ongoing rapid Arctic warming, retreating sea-ice, and intruding Atlantic waters in the Eurasian Basin (Mulwijk
et al., 2023), the perennial sea-ice that has remained in place still only permits one polar species to thrive: *N. pachyderma*.
Indeed, net samplings conducted between 1985 and 2015 showed that subpolar species of foraminifera are not yet increasing
335 in the region of the Fram Strait (Greco *et al.*, 2022). In fact, a decrease in subpolar species was found, which they linked to
the increased export of Arctic sea-ice through this narrow gateway (Greco *et al.*, 2022). It was hypothesized that the invasion
of the central Arctic Ocean by subpolar species will commence when ice export comes to a halt and the influence of Atlantic
waters in the central Arctic increases (i.e. ‘Atlantification’ *sensu* Polyakov *et al.*, 2017). The dataset presented here provides
an important baseline for comparison in future studies that will likely document this transformation. Of particular interest
340 will be tracking the response of *N. pachyderma* as seasonal sea-ice disappears.

4.2. Spatial patterns of *N. pachyderma* abundance

In order determine their controlling variables, planktonic foraminifera abundances are commonly compared (correlated) with
environmental parameters such as sea surface temperature (SST), sea surface salinity (SSS), chlorophyll *a*, and sea-ice cover
345 (area coverage in %). In the case of the perennially ice-covered central Arctic Ocean (*SAS ODEN21* sites), it should be noted
that both SST and SSS in the near-surface waters are strongly dictated by the ice pack, meaning that both SST and SSS were
virtually constant across our study sites (respectively ca. -1.7°C and 30 g/kg). Therefore, neither SST nor SSS were able to
explain the variability in concentration of *N. pachyderma* across the sites in the central Arctic Ocean. Similarly, the position
of the Atlantic water mass, as well as its maximal temperature (ca. 0.5°C), were extremely similar at 6 out of 8 stations (Figs.
350 4 and 5) indicating that they also do not contribute towards the observed variations in abundance across these sites. One
consideration to make is that the spatial distribution of planktonic foraminifera populations within a given area is well known
to exhibit ‘patchiness’ – meaning that populations are not distributed uniformly but can be characterised by marked



differences in their abundance (e.g. Boltovskoy, 1971). In our survey, we found that the variability in abundance in the central Arctic Ocean ranged between 18-65 ind. m⁻³ (average in top 200m, which points towards some degree of patchiness. 355 However, for sites that were located away at least 50 km away from the sea ice edge, we found a reasonable correlation between the chlorophyll *a* concentration (maximal value in the top 50 m) and concentration of *N. pachyderma* in the top 50 m of the water column (Fig. 9; linear fit $y = 641.44x - 93.624$, $r^2=0.79$). This implies that local variability in primary production (and thus food availability) may exert a dominant control on concentrations under ice-covered conditions. On the other hand, the correlation did not hold when taking into account sites that were located near the sea-ice edge (Fig. 9), 360 perhaps because other factors become dominant closer to the ice edge.

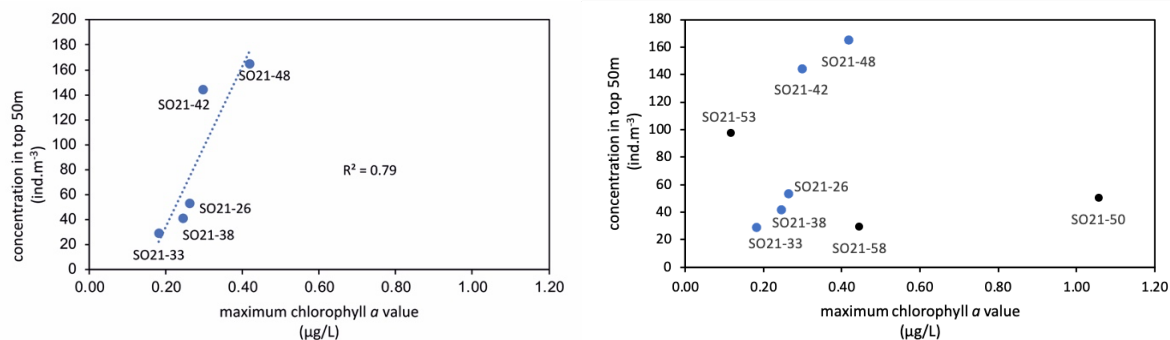
In terms of absolute abundance, the observed concentrations of *N. pachyderma* (range 7.8-27.5 ind/m³; averages in the top 500 m) are comparable to those reported at the ice-covered sites between 83°-86°N reported by Carstens and Wefer in 1992 (range 7.6-15.9 ind.m⁻³; averages in the top 500m). Based on these two studies alone, it could perhaps be suggested that this range of concentrations is typical for *N. pachyderma* under summer sea-ice, and that these have not markedly change in the 365 past 30 years. However, more studies are evidently needed to characterize both the spatial and temporal (seasonal/annual/decadal) trends of *N. pachyderma* concentrations in the central Arctic Ocean. In order to put these numbers in a broader perspective, we compared our results with concentrations reported near or outside of the seasonal ice edge, (re-)calculating the average in the top 200 m for these studies based on the original data (Table 2). The highest concentrations of *N. pachyderma* have been observed in open waters located near the ice margin, where values were one magnitude higher 370 than under sea ice (150-915 ind.m⁻³; Carstens and Wefer, 1997; Table 2). In the North Atlantic Ocean, the lowest concentrations observed along an East-West transect across the 75°N parallel (20 ind.m⁻³) were comparable to those found under sea-ice, but maximal concentrations were considerably higher (390 ind.m⁻³; Stangeew, 2001). Overall, these observations probably reflect broad-scale spatial changes in primary productivity in the ocean, which is known to reach its highest values in the marginal ice zone (Carstens et al., 1997).

In the region of the Lincoln Sea and adjoining fjords (*RYDER19*), abundances of planktonic foraminifera were extremely low, and are comparable to other studies reporting *N. pachyderma* concentrations in shelf environments (<2 ind.m⁻³; Kohfeld 375 et al., 1996; Zamelczyk et al., 2021). Common reasons to explain low abundances in (inner) shelf regions are the high variability in the physical and chemical environment, high turbidity and suspended sediment load, and shallow water depths impeding foraminifer reproduction cycles (Schmuker, 2000; Zamelczyk et al., 2021). We propose that limited food 380 availability, implied by the low levels of chlorophyll *a* near the surface are the likely cause for the low numbers of planktonic foraminifera in this region. Indeed, chlorophyll *a* concentrations are higher in the Lincoln Sea compared to Ryder Fjord, the latter exhibiting a narrower and deeper subsurface peak compared to the area outside the fjord (Fig. 10). This is consistent with the somewhat elevated foraminiferal abundances in the Lincoln Sea to outer Nares Strait region, compared to the very low abundances in Sherard Osborn Fjord (Fig. 6)



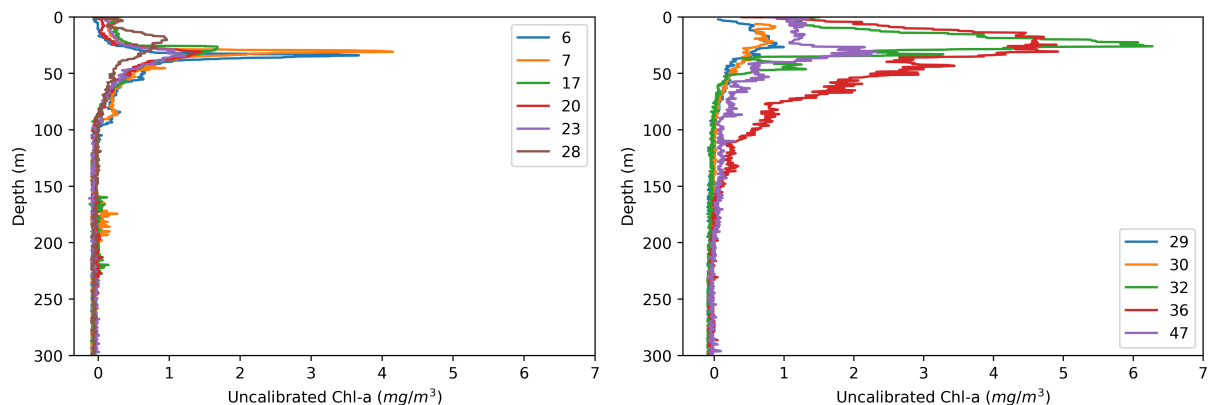
385 4.3. Depth habitat of *N. pachyderma*

Our results confirm earlier studies showing the shallow habitat of *N. pachyderma* underneath perennial sea ice (Bé, 1960; Carstens and Wefer, 1992; Volkmann, 2000). We speculate that the predominance of *N. pachyderma* in the upper 50 to 100 m in the central Arctic Ocean is related to food availability (presumably diatoms), which in turn depends on nutrient availability and light penetration limited by the presence of sea ice. Indeed, the chlorophyll *a* maximum is typically located
 390 between 20-40m, corresponding to the depth interval where the maximal concentration of tests typically occurs (Fig. 5). Moreover, the correlation between *N. pachyderma* abundance and chlorophyll *a*, found at sites located >50 km from the ice edge (Fig. 9), seems to imply a direct influence of primary productivity on the concentration of *N. pachyderma* at ice-covered sites with a thick layer of Polar Surface Water. The fact that the Polar Surface Water consists of cold and low salinity waters does not appear to hinder the resident *N. pachyderma* populations. These observations confirm previous
 395 suggestions that food availability/chlorophyll *a* concentration play a key role in determining the depth habitat of *N. pachyderma* (Kohfeld *et al.*, 1996; Volkmann, 2000; Pados & Spielhagen, 2014; Greco *et al.*, 2019) and that low salinity can be tolerated. This is further supported by the fact that highest abundances of *N. pachyderma* in the northern North Atlantic and Arctic Ocean ever reported were found in the highly productive marginal ice zone (Carstens and Wefer, 1997). Important to note is that a distinction should be made between the ‘main depth habitat’ of *N. pachyderma*, and the depth at
 400 which the secondary calcite is secreted, which is more important when it comes to interpreting geochemical signatures of fossil test in paleoceanography (Tell *et al.*, 2022). At all stations, test size increased from the surface to 100-200m depth, and at six out of eight stations no statistical difference was found between the 100-200 m and 200-500 m depth interval (Fig. 11; Fig. A4). This pattern would be consistent with gametogenesis taking place at the base of the productive zone, located at or below 100m, and would provide some evidence that *N. pachyderma* does perform ontogenetic vertical migration (Tell *et al.*,
 405 2022). On the other hand, large individuals were present at all depths, but rare (Fig. 11), perhaps substantiating that *N. pachyderma* performs both ontogenetic vertical migration as well as test growth at fixed depths, in line with the findings of Tell *et al.* (2022). Nevertheless, this result is to be confirmed and further analysed with a comprehensive analysis of *N. pachyderma* morphotypes in a follow-up study.





- 410 **Figure 9: Correlation between planktonic foraminifera abundance in the top 50 m and the corresponding maximum chlorophyll *a* value. Left shows only stations under heavy ice cover and far away from the sea-ice margin, right includes stations closer to the ice margin (Fig. 2). Blue dots indicate sites > 50km away from the ice margin, black dots indicate sites located within 50km of the ice margin.**



- 415 **Figure 10: Fluorescence-based estimate of chlorophyll *a* obtained during the *RYDER19* expedition. Left panel shows profiles obtained within the Fjord, right panel shows profiles obtained in the Lincoln Sea/Outer Nares Strait. Numbers indicate the names of the CTD stations, see Fig. 1 for their location.**

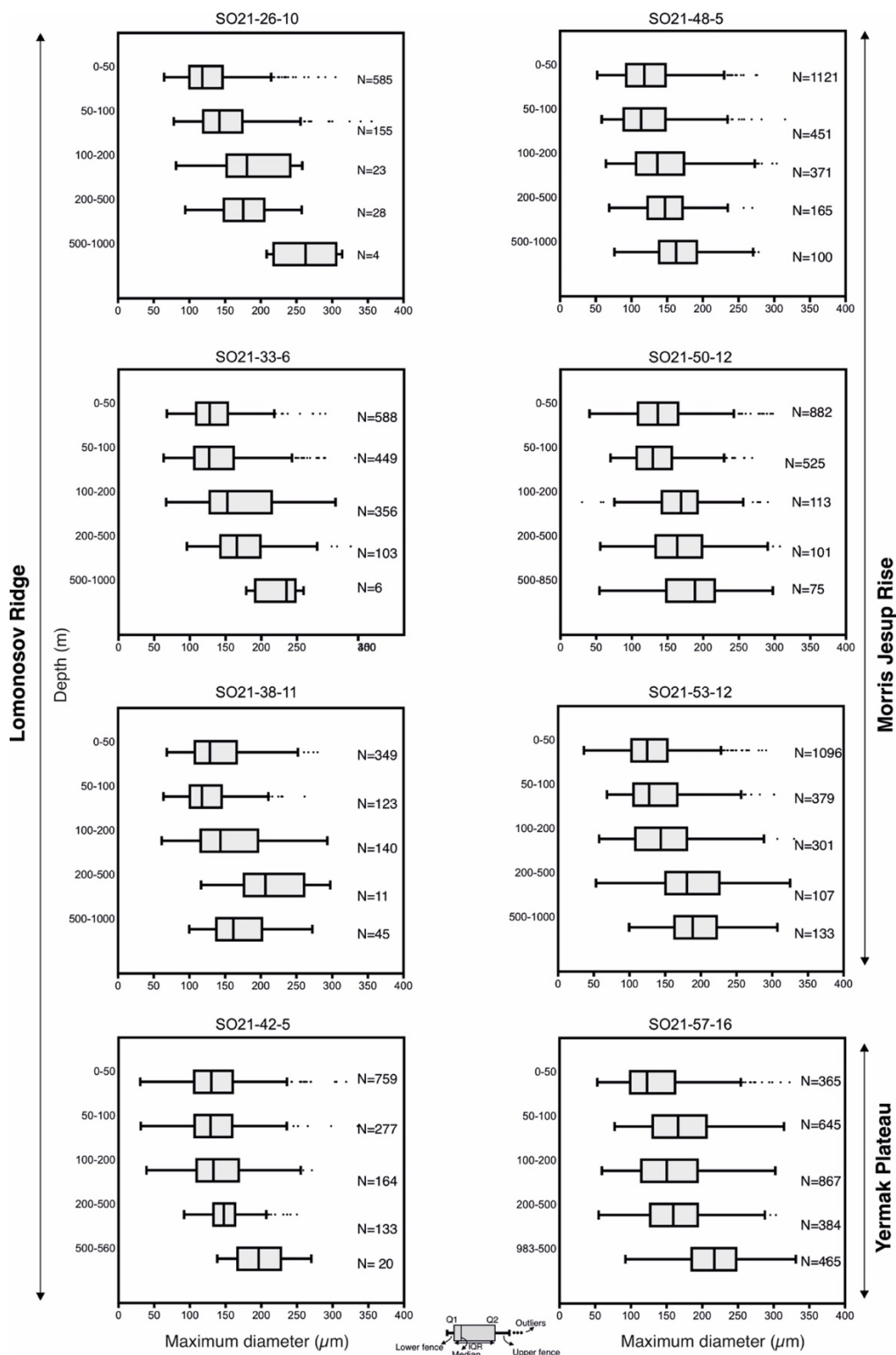




Fig. 11. Size distributions of planktonic foraminiferal tests obtained at each station and depth interval (SAS ODEN21).

420 5. Conclusion

This study details the first systematic survey of live planktonic foraminifera populations in the high Arctic Ocean (sites near the North Pole Area, southern Lomonosov Ridge, and the area north of Greenland). We document that *N. pachyderma* is the only species present underneath the perennial ice cover in the region between the North Pole–Greenland, and that sub-polar species have not migrated into the central Arctic Ocean. This is consistent with previous research showing that subpolar species are currently largely ‘blocked’ from entering the central Arctic due to increased sea-ice export through the Fram Strait (Greco et al., 2022). *Turborotalita quinqueloba* was only observed in very low numbers near the Yermak plateau and is absent at sites near the Lomonosov Ridge and the Lincoln Sea. This is consistent with its preference for Atlantic waters and abundance at/near the marginal ice zone, which has been widely reported. Overall, this observation emphasizes the prominent oceanographic and climatic changes that must have occurred in the region of the central Arctic Ocean during the Last Interglacial, where evidence for a large-scale *T. quinqueloba* invasion is apparent (Vermassen et al., 2023).

Underneath perennial sea ice, *N. pachyderma* prefers a shallow habitat (in the top 50 to 100m), in contrast to the ice marginal zone or areas with open water where it is more abundant at deeper water depths. We suggest that the shallow habitat is due to food availability, *i.e.*, phytoplankton in the photic zone. This is supported by a correlation of *N. pachyderma* concentration with chlorophyll-*a* concentrations at sites located well within the ice pack. The size distribution of *N. pachyderma* in the water column consistently revealed increasing test sizes with depth, with cytoplasm-bearing individuals dominating the upper 100m and empty tests dominating below 200m. This could perhaps represent a form of ‘ontogenetic vertical migration’, with individuals sinking as they grow, and reproducing around 100m water depth. However, encrusted specimens were observed at all depths (albeit it at very low percentages in the top 100m) and future studies deploying repeated tows would be needed to adequately determine the reproduction pattern of *N. pachyderma* under the summer sea ice.

As the Arctic Ocean is currently witnessing rapid environmental change, this dataset will provide an invaluable baseline for assessing the speed of change in the abundance and composition of planktonic foraminifera communities, in response to sea-



ice decline and ‘Atlantification’, which are anticipated to intensify in the coming decades. Also, the study can be used to enhance palaeoceanographic investigations that use the sedimentary record.

445 Table 1. Multinet sampling stations during SAS Oden 2021.

Expedition	Sampling		Depth (m)	Net (m)	Water depth (m)	Date	Time (UTC)	Type
	station	Latitude						
SAS ODEN21	SO21-26-10	89.126	-150.593	1000	1341	2021-08-19	23:38:00	Multinet
SAS ODEN21	SO21-33-6	88.143	-101.94	1000	2987	2021-08-25	16:27:00	Multinet
SAS ODEN21	SO21-38-11	87.747	-66.488	1000	1180	2021-08-28	23:29:00	Multinet
SAS ODEN21	SO21-42-5	86.519	-57.23	550	590	2021-08-30	23:09:00	Multinet
SAS ODEN21	SO21-48-5	84.927	-33.51	1000	1539	2021-09-03	19:30:00	Multinet
SAS ODEN21	SO21-50-12	84.16	-32.35	850	888	2021-09-05	01:22:00	Multinet
SAS ODEN21	SO21-53-4	84.462	-23.99	975	1350	2021-09-06	00:17:00	Multinet
SAS ODEN21	SO21-58-16	82.37	8.485	983	983	2021-09-11	10:42:00	Multinet
RYDER19	Ryder19-01-PN	82.344	-59.817	300	440	2019-08-09	N/A	Single net
RYDER19	Ryder19-02-PN	82.405	-56.254	300	448	2019-08-10	N/A	Single net
RYDER19	Ryder19-03-PN	82.024	-52.144	300	837	2019-08-14	N/A	Single net
RYDER19	Ryder19-04-PN	82	-52.227	408	836	2019-08-15	N/A	Single net
RYDER19	Ryder19-05-PN	81.884	-50.988	250	267	2019-08-21	N/A	Single net
RYDER19	Ryder19-06-PN	82.258	-52.814	300	372	2019-08-25	N/A	Single net
RYDER19	Ryder19-07-PN	82.477	-54.218	300	485	2019-08-26	N/A	Single net
RYDER19	Ryder19-08-PN	82.171	-59.806	300	420	2019-08-31	N/A	Single net



RYDER19	Ryder19-09-PN	81.64	-64.271	300	623	2019-09-02	N/A	Single net
RYDER19	Ryder19-10-PN	80.998	-60.974	300	1043	2019-09-03	N/A	Single net



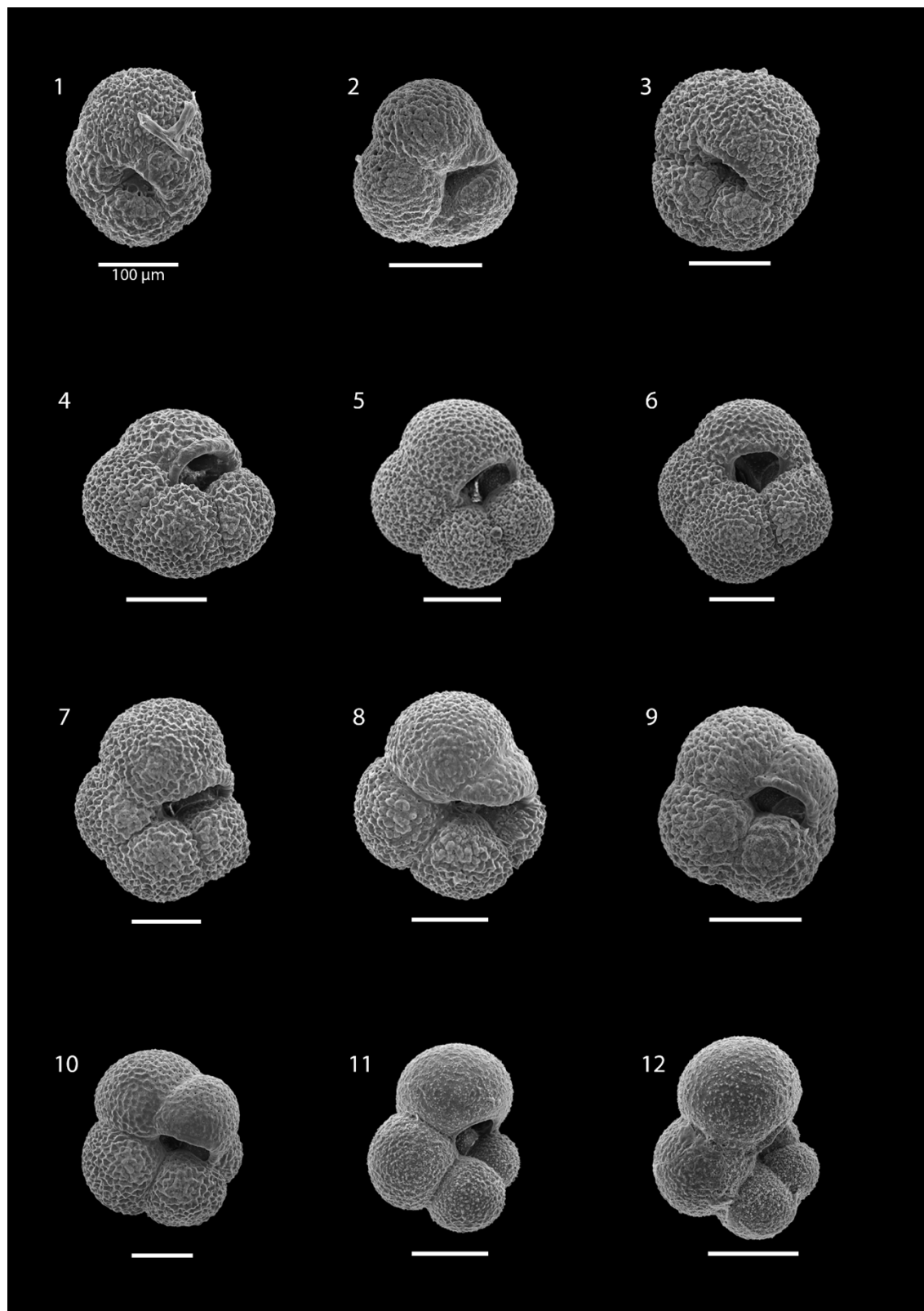
Table 2: Comparison of *N. pachyderma* concentrations (ind.m⁻³) across different sites in the northern North Atlantic

Region	Sub region	Latitude	Top 200m range or average (ind.m ⁻³)	Net size (µm)	Season	Ice conditons	Study
Arctic Ocean (>80N)							
	Lomonosov Ridge	86.5-89N	20-60	>63	Summer	ice-covered	This study
	Morris Jesup Rise	84.5-85N	20-65	>63	Summer	ice-covered	This study
	Lincoln Sea/Sherard Osborn Fjord	81-82N	0.15-0.30	>63	Summer	locally open waters	This study
	Nansen Basin	83-86N	140	>63	Summer	ice-covered	Carstens & Wefer (1992)
	Nansen Basin	81-83N	140	>63	Summer	ice-covered	Carstens & Wefer (1992)
	Yermak Plateau	82N	30	>63	Summer	ice-covered	This study
Fram Strait							
		80N	5-15	>63	Summer	ice-covered	Carstens & Wefer (1997)
		78N	665	>63	Summer	ice margin	Carstens & Wefer (1997)
		78N	150-915		Summer	open water	Carstens & Wefer (1997)
Northeast Greenland							
	NEW polynya	80.5N	0.25-20	150	Summer	polynya	Kohfeld & Fairbanks (1996)
Barents Sea							
		76-82N	<2	63	Winter	ice-covered	Zamelczyk et al. (2021)
North Atlantic	Nordic Seas	75N	20-390	63	Summer	open water	Stangeew (2001)



Plate 1. SEM images illustrating the various morphotypes of *N. pachyderma*.

1-3) Morphotype 'Nps-1'. 4-6). Morphotype 'Nps-2' 7-9). Morphotype 'Nps-3'. 10) Morphotype 'Nps-4'. 11-12)
Morphotype 'Nps-5'. Specimens 1, 3, 5, 6, 7, and 8 are from the 200-100m depth interval at station SO21-58-16. Specimens
455 2, 9, and 10 are from the 850-500m depth interval at SO21-50-12- specimen 4 is from the depth interval 200-100m at SO21-
50-12. Specimens 11 and 12 are from depth interval 50-0m at station SO21-50-12. All scale bars are 100 μm , unless
otherwise indicated.

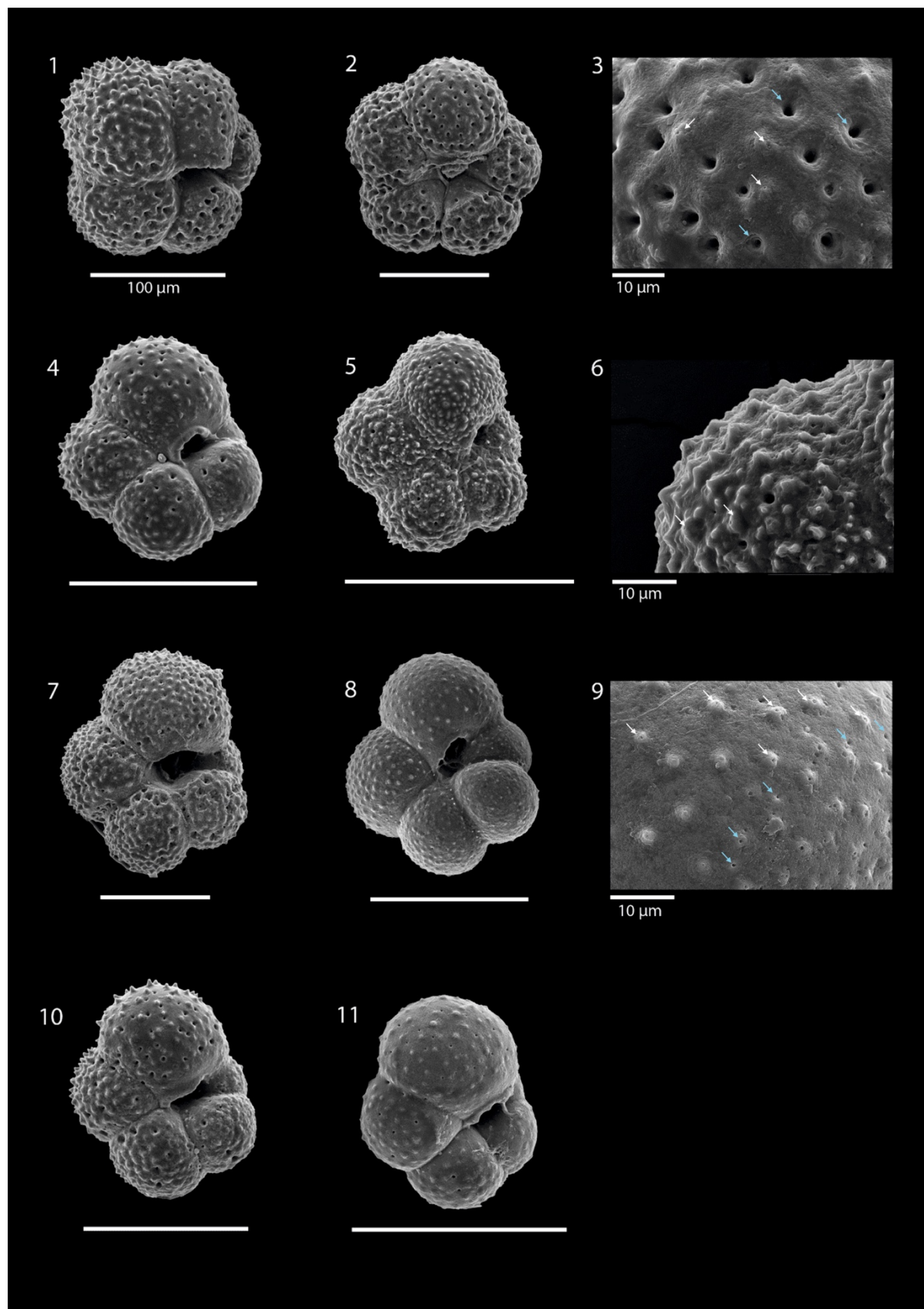




465

Plate 2 *Turborotalita quinqueloba*

Fig 1. Sample SO21-58-16, 500-200 m. Figs. 2, 4-11 Sample SO21-58-16, 200-100 m. Fig. 3 Wall texture of Figure 2. Fig. 6 Wall texture of Figure 5. Fig. 9 Wall texture of Figure 8. White arrows indicate spine holes, blue arrows indicate pores.





470 **References**

- Bé, A.W.** (1960) Some observations on arctic planktonic foraminifera. *Contrib. from Cushman Found. Foraminifer. Res.*, **11**, 64–68.
- Boltovskoy, E.** (1971) Patchiness in the distribution of planktonic foraminifera. In: *Proceedings of the 2. Planktonic Conference, Ed. Tecnoscienza, Rome, Italy*, 107–115.
- 475 **Brandt, S., Wassmann, P. and Piepenburg, D.** (2023) Revisiting the footprints of climate change in Arctic marine food webs: An assessment of knowledge gained since 2010. *Front. Mar. Sci.*, **10**, 1–17.
- Carstens, J., Hebbeln, D. and Wefer, G.** (1997) Distribution of planktic foraminifera at the ice margin in the Arctic (Fram Strait). *Mar. Micropaleontol.*, **29**, 257–269.
- 480 **Carstens, J. and Wefer, G.** (1992) Recent distribution of planktonic foraminifera in the Nansen Basin, Arctic Ocean. *Deep. Res.*, **39**, 507–524.
- Darling, K.F. and Wade, C.M.** (2008) The genetic diversity of planktic foraminifera and the global distribution of ribosomal RNA genotypes. *Mar. Micropaleontol.*, **67**, 216–238.
- Eynaud, F., Cronin, T.M., Smith, S.A., Zaragosi, S., Mavel, J., Mary, Y., Mas, V. and Pujol, C.**
485 (2009) Morphological variability of the planktonic foraminifer *Neogloboquadrina pachyderma* from ACEX cores: Implications for Late Pleistocene circulation in the Arctic Ocean. *Micropaleontology*, **55**, 101–116.
- Greco, M., Jonkers, L., Kretschmer, K., Bijma, J. and Kucera, M.** (2019) Depth habitat of the planktonic foraminifera *Neogloboquadrina pachyderma* in the northern high latitudes explained by
490 sea-ice and chlorophyll concentrations. *Biogeosciences*, **16**, 3425–3437.
- Greco, M., Werner, K., Zamelczyk, K., Rasmussen, T.L. and Kucera, M.** (2022) Decadal trend of plankton community change and habitat shoaling in the Arctic gateway recorded by planktonic foraminifera. *Glob. Chang. Biol.*, **28**, 1798–1808.
- Heuzé, C., Karam, S., Muchowski, J., Padilla, A., Stranne, C., Gerke, L., Tanhua, T., Ulfso, A.,
495 Laber, C. and Stedmon, C.A.** (2022a) Physical Oceanography during ODEN expedition SO21 for the Synoptic Arctic Survey.
- Heuzé, C., Karam, S., Muchowski, J., Padilla, A., Stranne, C., Gerke, L., Tanhua, T., Ulfso, A.,
Laber, C. and Stedmon, C.A.** (2022b) Physical Oceanography measured on bottle water samples during ODEN expedition SO21 for the Synoptic Arctic Survey.



- 500 **Hsiang, A.Y., Nelson, K., Elder, L.E., Sibert, E.C., Kahanamoku, S.S., Burke, J.E., Kelly, A., Liu, Y. and Hull, P.M.** (2017) AutoMorph: Accelerating morphometrics with automated 2D and 3D image processing and shape extraction. *Methods Ecol. Evol.*, **9**, 605–612.
- Jakobsson, M., Mayer, L., Farrell, J. and RYDER19 Scientific Party** (2020a) Expedition report: SWEDARCTIC Ryder 2019. Luleå.
- 505 **Jakobsson, M., Mayer, L.A., Nilsson, J., Stranne, C., Calder, B., O'Regan, M., Farrell, J.W., Cronin, T.M., Brüchert, V., Chawarski, J., Eriksson, B., Fredriksson, J., Gemery, L., Glueder, A., Holmes, F.A., Jerram, K., Kirchner, N., Mix, A., Muchowski, J., Prakash, A., Reilly, B., Thornton, B., Ulfso, A., Weidner, E., Åkesson, H., Handl, T., Ståhl, E., Boze, L.G., Reed, S., West, G. and Padman, J.** (2020b) Ryder Glacier in northwest Greenland is shielded from warm
- 510 Atlantic water by a bathymetric sill. *Commun. Earth Environ.*, **1**, 1–10.
- Kandiano, E.S. and Bauch, H.A.** (2002) Implications of planktic foraminiferal size fractions for the glacial-interglacial paleoceanography of the polar North Atlantic. *J. Foraminifer. Res.*, **32**, 245–251.
- Kohfeld, K.E., Fairbanks, R.G., Smith, S.L. and Walsh, I.D.** (1996) Neogloboquadrina pachyderma
- 515 (sinistral coiling) as paleoceanographic tracers in polar oceans: Evidence from Northeast Water Polynya plankton tows, sediment traps, and surface sediments. *Paleoceanography*, **11**, 679–699.
- Meier, W.N. and Stroeve, J.** (2022) AN UPDATED ASSESSMENT OF THE CHANGING ARCTIC SEA ICE COVER. *Oceanography*, **35**, 10–19.
- Nilsson, J., van Dongen, E., Jakobsson, M., O'Regan, M. and Stranne, C.** (2023) Hydraulic
- 520 suppression of basal glacier melt in sill fjords. *Cryosph.*, **17**, 2455–2476.
- Pados, T. and Spielhagen, R.F.** (2014) Species distribution and depth habitat of recent planktic foraminifera in Fram Strait, Arctic Ocean. *Polar Res.* doi: 10.3402/polar.v33.22483
- Polyakov, I. V., Pnyushkov, A. V., Alkire, M.B., Ashik, I.M., Baumann, T.M., Carmack, E.C., Goszczko, I., Guthrie, J., Ivanov, V. V., Kanzow, T., Krishfield, R., Kwok, R., Sundfjord, A.,**
- 525 **Morison, J., Rember, R. and Yulin, A.** (2017) Greater role for Atlantic inflows on sea-ice loss in the Eurasian Basin of the Arctic Ocean. *Science (80-.)*, **356**, 285–291.
- Rudels, B., Marnela, M. and Eriksson, P.** (2008) Constraints on Estimating Mass, Heat and Freshwater Transports in the Arctic Ocean: An Exercise. In: *Arctic--Subarctic Ocean Fluxes: Defining the Role of the Northern Seas in Climate* (Ed. R.R. Dickson, J. Meincke, and P. Rhines),
- 530 *Springer Netherlands*, Dordrecht, 315–341.



- Schiebel, R. and Hemleben, C.** (2017) Planktic foraminifers in the modern ocean. *Springer*, Berlin, 1–358 pp.
- Schmuker, B.** (2000) The influence of shelf vicinity on the distribution of planktic foraminifera south of Puerto Rico. *Mar. Geol.*, **166**, 125–143.
- 535 **Snoeijs-Leijonmalm, P.** (2022) Expedition Report SWEDARCTIC Synoptic Arctic Survey 2021 with icebreaker Oden. 300 pp.
- Stranne, C., Nilsson, J., Muchowski, J. and Chawarski, J.** (2020) Oceanographic CTD data from the Ryder 2019 expedition. In: Bolin Cent. Database. <https://doi.org/10.17043/oden-ryder-2019-ctd-1>.
- 540 **Tell, F., Jonkers, L., Meilland, J. and Kucera, M.** (2022) Upper-ocean flux of biogenic calcite produced by the Arctic planktonic foraminifera *Neogloboquadrina pachyderma*. *Biogeosciences*, **19**, 4903–4927.
- Vermassen, F., O'Regan, M., de Boer, A., Schenk, F., Razmjooei, M., West, G., Cronin, T.M., Jakobsson, M. and Coxall, H.K.** (2023) A seasonally ice-free Arctic Ocean during the Last Interglacial. *Nat. Geosci.*, **16**, 723–729.
- 545 **Volkman, R.** (2000) Planktic foraminifers in the outer Laptev Sea and the Fram Strait - Modern distribution and ecology. *J Foraminifer Res.* doi: 10.2113/0300157
- Zamelczyk, K., Fransson, A., Chierici, M., Jones, E., Meilland, J., Anglada-Ortiz, G. and Lødemel, H.H.** (2021) Distribution and Abundances of Planktic Foraminifera and Shelled Pteropods During the Polar Night in the Sea-Ice Covered Northern Barents Sea. *Front. Mar. Sci.*, **8**, 1–19.
- 550

Acknowledgements

We thank the crews and captains of IB Oden for skilfully operating the ship during both expeditions. The Polar Research Secretariat (SPRS) is thanked for assistance with handling of scientific equipment and expedition organisation. The scientific leadership of the expeditions SAD ODEN21 (Pauline Snoeijs-Leijonmalm) and RYDER19 (Martin Jakobsson, Larry Mayer) are thanked for planning and coordination of the expeditions.

555

Funding

FV is supported by the Formas mobility grant for early-career researchers, grant nr 2022-02861. HC and FV acknowledge funding from VR grant DNR 2019-03757. CH and SK acknowledge funding from the Swedish Research Council



560 (Vetenskapsrådet) Starting Research Grant (2018-03859). AH is supported by the Swedish Research Council
(Vetenskapsrådet) Starting Research Grant (ÄR-NT 2020-03515).

Author contributions

FV, CB, and HC designed the study. FV led the analysis and wrote the manuscript. FV and CB collected the foraminiferal data with the help of TW and AH. HF, CH, SK, CS, and MS collected and provided the environmental data. All authors
565 contributed to the writing and revising of the manuscript.

Data availability

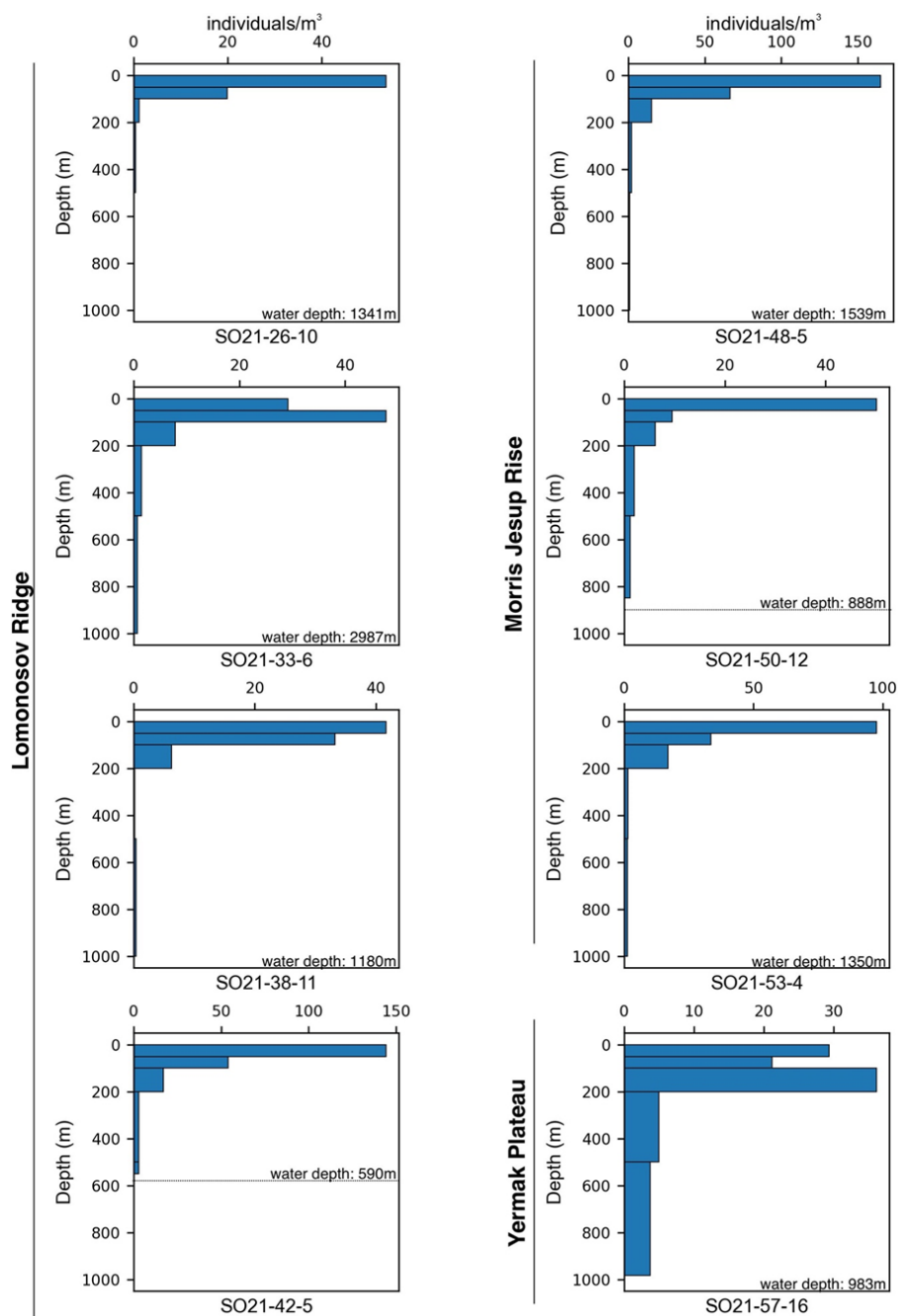
The foraminiferal data related to this article is submitted and under revision at the Bolin Centre database to be made available for open access.

570 **Competing interests**

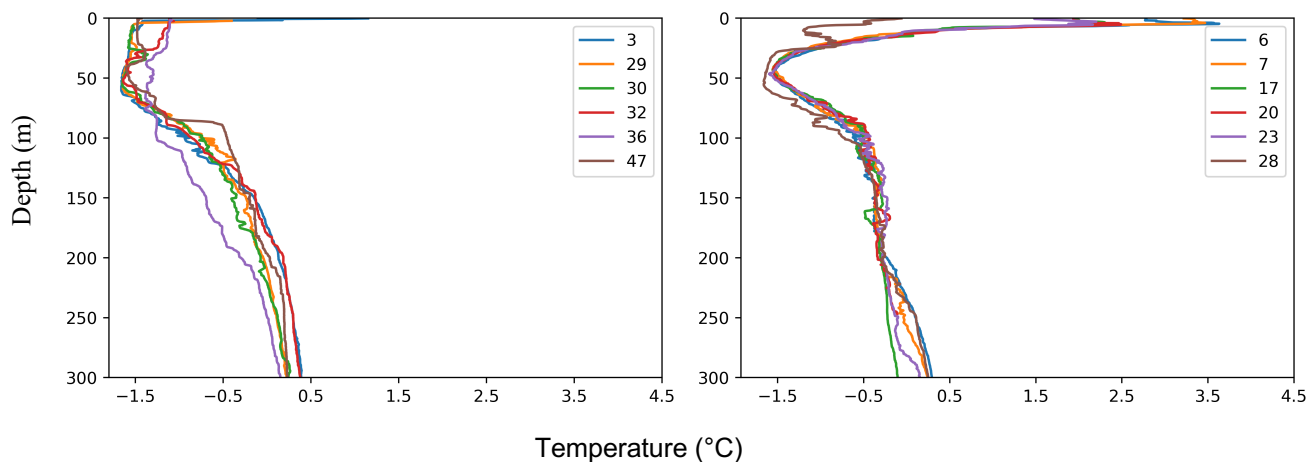
The authors have no competing interests to declare.



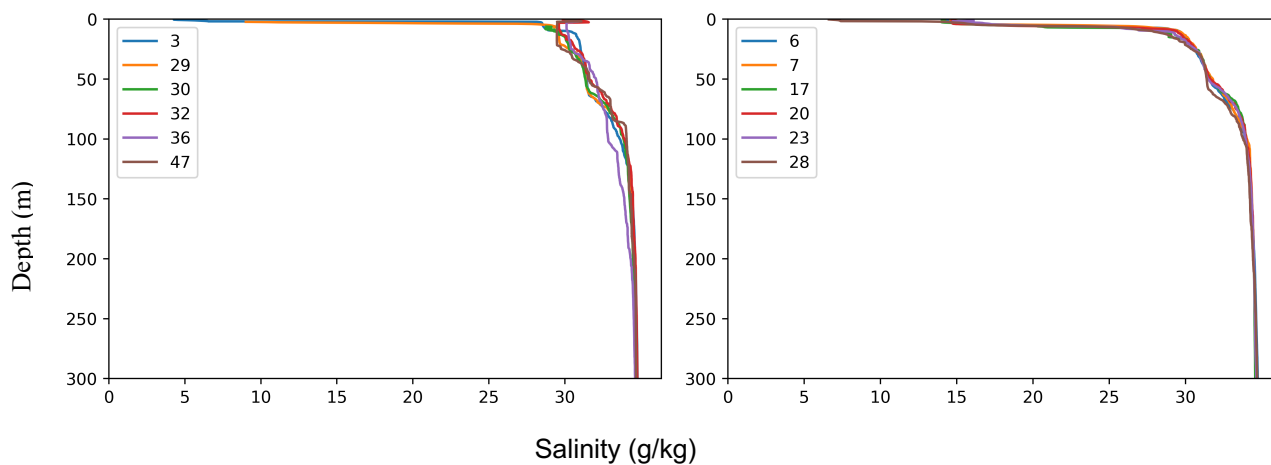
Appendix



575 Figure A1. Planktonic foraminifer abundances at each site of SAS ODEN 21 (full depth down to 1000m)



580 Figure A2: Temperature profiles in the Lincoln Sea and outer Nares Strait (Left) and Sherard Osborn Fjord (Right)



585 Figure A3: Salinity profiles in the Lincoln Sea and Nares Strait (Left) and Sherard Osborn Fjord (Right)



		500-1000	200-500	100-200	50-100	0-50
SO21-26-10	500-1000				1,355E-	
	1000		0,0003304	0,007835	06	0
	200-500	5,893		0,6696	0,3103	8,63E-07
	100-200	4,721	1,888		0,005512	0
	50-100	7,52	2,708	4,865		0
	0-50	9,66	7,639	9,451	10,2	

		500-1000	200-500	100-200	50-100	0-50
SO21-33-6	500-1000		0,1004	0,02613	8,19E-05	3,091E-05
	1000				2,681E-	
	200-500	3,481		0,5153	12	0
	100-200	4,185	2,224		8,511E-	
	50-100	6,333	10,44	9,771	11	1,956E-12
	0-50	6,629	11,11	10,49	1,747	0,7305

		500-1000	200-500	100-200	50-100	0-50
SO21-38-11	500-1000		0,05563	0,4578	1,351E-	
	1000				06	0,000188
	200-500	3,812			8,505E-	
	100-200	2,352	5,382	0,001449	08	2,827E-06
	50-100	7,535	8,246		2,563E-	
	0-50	6,085	7,335	5,606	06	0,0007759
						0,1297

		500-560	200-500	100-200	50-100	0-50
SO21-42-5	500-560		2,262E-07	6,712E-	0	0



			10		
200-500	7,953		0,5258	0,008177	0,001704
100-200	9,305	2,201		0,4422	0,2939
50-100	10,78	4,696	2,386		1
0-50	11,12	5,307	2,751	0,02578	

SO21-48-5	500-1000	200-500	100-200	50-100	0-50
500-1000				6,144E-	
1000		0,03626	0,001007	11	6,145E-11
200-500	4,023		0,9236	4,671E-	1,019E-10
100-200	5,491	1,164		6,224E-	
50-100	12,34	9,384	10,63	11	6,145E-11
0-50	12,76	9,863	11,91	0,563	

SO21-50-12	500-850	200-500	100-200	50-100	0-50
500-850				1,555E-	
200-500	4,225	0,02385	0,06432	12	1,554E-12
100-200	3,729	0,6467		4,23E-10	2,447E-08
50-100	13,48	9,39	10,69	2,172E-	
0-50	12,76	8,481	9,803	12	6,044E-11
					0,4594
				2,347	

Figure A4: Results of Tukey's pairwise comparison, performed on the maximal diameter data, calculated for each station. Numbers above the diagonal indicate p values, numbers below the diagonal indicate Tukey's Q value. Numbers highlighted in yellow indicate pairs that are not statistically significant from each other.